

OBSERVATION OF LIQUID METAL ACTUATION IN MICROFLUIDIC
CHANNELS AND IMPLEMENTATION TO TUNABLE RF INDUCTORS

A Thesis

by

YUSUF DOGAN

Submitted to the Office of Graduate and Professional Studies of
Texas A&M University
in partial fulfillment of the requirements for the degree of

MASTER OF SCIENCE

Chair of Committee,	Arum Han
Committee Members,	Gregory Huff
	Jim Xiuquan Ji
	Choongho Yu
Head of Department,	Chanan Singh

August 2014

Major Subject: Electrical Engineering

Copyright 2014 Yusuf Dogan

ABSTRACT

The overarching goal of this thesis research is to analyze liquid metal plug actuation in microfluidic channels and to exemplify this actuation in a tunable inductor design using liquid metal as a switching material, and to demonstrate the feasibility of liquid metal in other devices.

A gallium and indium based alloy, EGaIn, which is liquid at room temperature is the liquid metal type chosen for this research. Although it owns some advantages such as high vapor pressure, non-toxicity and good conductivity, there are some crucial factors that we should pay attention to move the liquid metal in microchannels as a result of oxidation with contact to air and stickiness of oxidized skin to any surface. One of them is to determine the right coating material for coating the channel and the best surfactant to carry the liquid metal plug without leaving residues with sufficient amount of pressure.

So far, liquid metals have been used in some RF applications, but EGaIn could not be implemented properly in a microfluidic channel as a separate liquid metal plug because of the oxidation issue. Our aim is here to verify that there are ways to handle the actuation of based liquid metals in microchannels. In this thesis, we have used EGaIn in the experiments conducted, but the acquired results are also applicable to galinstan, which is another gallium based alloy.

Right after the liquid metal actuation is exhibited in microfluidic channels, this actuation is exemplified in tunable loop and spiral inductors on both PCB and glass

slides using lithography technique. A closed loop channel with peristaltic pumping valves has been designed with the help of LabVIEW™ and proper channel designing technique. Therefore, moving the liquid metal in a desired way with an expected speed is achieved.

At the end of the study, tunability in an RF inductor using liquid metal as a switching part is provided, once a solution to the nagging oxidation problem of liquid metals is offered, and thus the feasibility of liquid metals to the electrical device applications is demonstrated.

DEDICATION

As a gift to the gift of my life,

All my works are dedicated to you, my beloved wife.

ACKNOWLEDGEMENTS

I would like to express my deepest gratitude to my advisor and committee chair, Dr. Arum Han, who have changed the course of my academic career. Without his guidance and persistent help this thesis would not have been possible. I would also like to thank my committee members, Dr. Gregory Huff, Dr. Jim Xiuquan Ji, and Dr. Choongho Yu, for providing advice, information and support on different aspects of my thesis.

I am greatly indebted to my NanoBio Systems lab mates, and my special thanks goes to Dr. Chiwan Koo, Dr. Jaewon Park, Dr. Sungman Kim, Hyun Soo Kim, Han Wang, Celal Erbay, Adrian R. Guzman, Sehoon Jeong, Sergio C. Waqued, Nebras Sobahi and Keith Krenek, who have given me constructive comments and warm encouragement. Discussions with them have been illuminating to me. I have always been proud of being a part of NanoBio Systems Lab. And, I would like to extend my appreciations to Dr. Gregory Huff and Michael Kelley from Electromagnetic Field Lab for sharing their laboratory and equipment. I owe thanks to my friends, colleagues, and the department faculty and staff for the great experiment I have in Texas A&M University.

Words cannot express how grateful I am to my mother, father, sisters, brothers-in-law, parents-in-law, sisters-in-law and my nephew and niece who have been a source of encouragement and inspiration to me. Their prayer for me was what sustained me thus far. Most of all, I would like to express appreciation to my beloved wife Sumeyra, who

conveyed an excitement in regard to being by me in all the processes of building my thesis. Her support on research as well as on my career has been priceless to me.

NOMENCLATURE

LM	Liquid Metal
EGaIn	Eutectic Gallium Indium
RF	Radio Frequency
HCl	Hydrochloric Acid
PCB	Printed Circuit Board
PDMS	Polydimethylsiloxane
PTFE	Polytetrafluoroethylene
HFSS	High Frequency Structural Simulator
IPA	Isopropyl Alcohol

TABLE OF CONTENTS

	Page
ABSTRACT	ii
DEDICATION	iv
ACKNOWLEDGEMENTS	v
NOMENCLATURE.....	vii
TABLE OF CONTENTS.....	viii
LIST OF FIGURES	x
LIST OF TABLES	xiii
1. INTRODUCTION	1
1.1 Objective and Motivation	1
1.2 Liquid Metal and Properties	2
1.3 Conventional Liquid Metal Actuation.....	6
1.4 Application of Liquid Metals in RF Components	7
2. LIQUID METAL ACTUATION IN MICROFLUIDIC CHANNELS	10
2.1 Actuation of Liquid Metal in Straight Channel.....	11
2.1.1 Design and Fabrication	11
2.1.2 Effective Microchannel Coating.....	12
2.1.3 Effective Surfactant for Liquid Metal Carriage.....	17
2.1.4 Optimizing Channel Dimensions and Liquid Metal Sizes.....	19
2.2 Actuation of LM in Closed Loop Channel	26
2.2.1 Design and Fabrication	26
2.2.2 Experimental Steps and Results.....	30
3. LIQUID METAL IN MICROFLUIDIC TUNABLE INDUCTOR.....	34
3.1 Design and Fabrication of RF Switch	34
3.2 Design and Fabrication of Tunable Loop Inductor	39
3.3 Tunable Spiral Inductor on PCB	44
3.3.1 Spiral Inductor Design with Straight Channel.....	44

	Page
3.3.2 Spiral Inductor Design with Closed Loop Channel	48
4. SUMMARY AND FUTURE WORK.....	51
4.1 Summary.....	51
4.2 Future Work.....	52
REFERENCES.....	54
APPENDIX A	58
APPENDIX B	62
APPENDIX C	64
APPENDIX D.....	67

LIST OF FIGURES

	Page
Figure 1 3D Straight Channel Master Mold, Inverted Replica of PDMS and Whole Device.....	12
Figure 2 The Setup for Surfactant Test Analysis.....	17
Figure 3 Liquid Metal in Different Channel Dimensions.....	20
Figure 4 Images of EGaIn Plug in Different Channel (w/h) Ratios a) View of EGaIn Plug in the Channel Whose w/h Ratio Is 2, b) View of EGaIn Plug in the Channel Whose w/h Ratio Is 8.....	21
Figure 5 Minimum Required Flow Rate/ Cross Sectional Area to Channel Dimension Ratios	22
Figure 6 Images of Two Different Size EGaIn Plugs in the Same Channel (Width Is 500 μ m) a) A Short Plug (l/w: 2), and b) A Long Plug (l/w: 12).....	23
Figure 7 Images of EGaIn Plugs in Different Lengths in the Same Channel (Channel Width Is 2000 μ m) a) The Plug Is Short Enough to Move, and b) The Plug Is Longer Than the Threshold Length.....	24
Figure 8 Effective Liquid Metal Length to Channel Width Ratio (Channel Width Is 500 μ m). If the l/w Ratio Is Between 1 and 8, Flow Rate/Cross Sectional Area of Channel Is Minimum for Actuating Liquid Metal. In the l/w Ratio Other Than This Range, the Plug Does Not Move.....	24
Figure 9 Effective L/W Ratio for Actuating Liquid Metal with Given Channel Widths as 500 μ m, 1000 μ m, and 2000 μ m Respectively.....	25
Figure 10 Overall Closed Loop Design.....	27
Figure 11 The Working Principle of Peristaltic Pump with Microvalves	28
Figure 12 Fabrication Steps of Closed Loop Device.....	29
Figure 13 The Overall Setup for LM Actuation in Closed Loop Device with the Solenoid Valve Controller.....	30

	Page
Figure 14 Images of EGaIn Plug under the Valves and after LM Passage	31
Figure 15 Designs of Different Closed Loop Devices a) Design with Only One Sequential Pumping, and b) Design with Secondary Sequential Pumping.....	32
Figure 16 Images of LM Movement in Closed Loop Device with Respect to Time	32
Figure 17 S Parameters of Matching Network	34
Figure 18 RF Switching Device and Fabrication Steps.....	35
Figure 19 OFF State S_{21} Forwarded Gain of the RF Switch with Different Surfactants.....	36
Figure 20 ON State S_{21} Forwarded Gains of RF Switch with Different Surfactants	37
Figure 21 Dielectric Constants of Diluted PTFE Solutions.....	37
Figure 22 Loss Tangent of Different Percentages of PTFE Dilution	38
Figure 23 Tunable Loop Inductor Design a) Fabrication Process of the Inductor Patterned on a Glass Slide, b) Channel Layers, and c) Overall Device	40
Figure 24 Two Different Inductor Designs a) Type 1 Tunable Inductor Design b) Type 2 Tunable Inductor Design.....	42
Figure 25 Inductance Result Graphics of Tunable Inductors a) Results of Type 1 Tunable Loop Inductor, and b) Results of Type 2 Tunable Loop Inductor ...	43
Figure 26 Illustration of the Overall Design of PCB Tunable Spiral Inductor with Straight Channel	44
Figure 27 Fabrication Steps of PCB Inductor Design	45
Figure 28 a) E-Field Distribution of Simulated PCB Inductor While Long Inductor Is ON b) Fabricated PCB Inductor Design with Straight Channel	46
Figure 29 Simulated and Measured Results of Spiral Inductor a) Inductance of Simulated and Measured Short Inductor, and b) Inductance of Simulated and Measured Long Inductor	47
Figure 30 Illustration of PCB Inductor Design with Closed Loop Channel.....	48

	Page
Figure 31 Fabrication Process of Closed Loop Device on PCB.....	49
Figure 32 Fabricated Closed Loop Device	50

LIST OF TABLES

	Page
Table 1 Prominent Properties of Liquid Metals	2
Table 2 Images of Sticking Residue on Channel Surfaces after LM Actuation.....	14
Table 3 Different Percentages of PTFE and Thermo-Treatment Effects on PDMS Channel Roughness	16
Table 4 Left Residue Inside the Microfluidic Channels after LM Actuation 1 st , 3 rd and 5 th Times Respectively	18

1. INTRODUCTION

1.1 Objective and Motivation

Examining the LM related literature and history; one can readily assume the crucial role of LM in the scientific improvements of the recent past and the day. The outstanding properties have made LM the focal point of many studies. As the liquid metals carry the features of both metals like conductivity and high density, and liquids like formlessness and fluidity they are quite promising for the future studies. It is a necessity to overcome any problem hindering the LM applications and development of devices employing LM for the future projects that are expected to bring great progress in technology.

In this thesis, my efforts will be intended to offer some solutions to handle the obstacles of using LM actuation. If I specify the objectives of this thesis, they are: (1) to solve the matter of adhesion of LM to the channel walls and find a better coating material helping to achieve this, (2) to observe actuation of LM over time and under various conditions, (3) to find the best surfactant to move the LM plug without leaving residues, (4) to optimize the channel size and LM size in the microfluidic channel, (5) to employ peristaltic pumping mechanism on closed loop channel device for actuating the LM plug, (6) to get a good RF switching performance recurrently, and finally (7) to demonstrate the compatibility of LM in microchannels with tunable RF inductors.

Once these objectives are achieved at the end of the study, what is to be acquired is a clear LM carriage in microchannel and getting a high tuning range with a good

quality factor in a tunable inductor that uses LM actuation as a switching mechanism. This tunable inductor will just be an example of successful liquid metal actuation. When we will succeed in this project it is supposed to offer an insight into similar applications and further future studies.

1.2 Liquid Metal and Properties

Liquid metal is a formless metal, which is liquid at room temperature. LMs have remarkable mechanical properties like large surface tension and low viscosity. [1] Besides, they have a high degree of thermal conductivity superior to ordinary liquids and inherent high densities and electrical conductivities. [2] Mercury, field's metal, rose's metal, wood's metal and gallium based alloys are the types of LM available for studies. Most commonly used gallium based alloys are galinstan and EGaIn. All these liquid metals possess different properties and values. Table 1 depicts some values of the liquid metal types and provides us making a comparison among them.

Liquid Metals	Electrical Conductivity (S*10 ⁶ /m)	Melting temperature (°C)	Density (g/cm ³)	Solubility in water or organic solvents	Viscosity at 20°C (Pas)	Vapor pressure (Torr)
Galinstan	3.46	-19	6.44	No	0.0024	1e-8
EGaIn	3.4	15.78	6.25	No	0.002	NA
Mercury	1	-38.87	13.55	No	0.0015	1.68e-3
Copper	59.6	1085	8.96	-	-	-

Table 1: Prominent Properties of Liquid Metals.

It is obvious that mercury as a liquid metal was widely used in older studies. Mercury was preferable because it is a good conductor of heat, it has a uniform

expansion and it is easily available in pure state. According to Kim *et al*, mercury's low contact resistance and its lack of signal bounce greatly increase the instruments' performance, and in micro scale, mercury droplets show a great physical stability since inertial forces become negligible while surface tension force gains its importance. [3] However, as it exerts low vapor pressure and was proved to be poisonous, some alternative liquid metals have begun to be considered.

Field's metal, an alternative LM alloy, consists of 32.5% bismuth, 51% indium and 16.5% tin, and it is a non-toxic material. It is safe to use because it does not contain lead or cadmium. Field's Metal is generally used for casting. Moreover, it is solid at room temperature, and this makes it ideal for making 3D electrodes for micro devices at room temperature. Nevertheless, the temperature should be above 65°C if we want to move it as a liquid.

Rose's metal is comprised of 50% bismuth, 25-28% lead and 22-25% tin. Its melting point is between 94°C and 98°C, which makes it not practicable for applications intended to actuate and flow it as a liquid metal. It is generally used as a solder and heat transfer material.

Wood's metal, another type of LM alloy, consists of 50% bismuth, 26.7% lead, 13.3% tin and 10% cadmium. It is known to be useful as a solder, casting material, high temperature coupling fluid and a heat transfer material. Similar to the last two alloys, it has a high melting point, which is approximately 70°C. Therefore, it is not applicable for our study or the other studies in the same direction.

Galinstan, on the other hand, is a nontoxic and very low vapor pressure inclusive metal alloy that composed of 68.5 % gallium, 21.5 % indium and 10 % tin. [4] Galinstan is now used in many applications like cooling for microelectronics because of its thermophysical properties [5], RF MEMs switch [6], and patch antenna making use of the stretchability of encapsulated galinstan with elastomer. [7]

EGaIn is a commercially available liquid metal made up of 75% gallium and 25% indium. [8] Having a high surface tension and high electrical conductance are the prominent characteristic of EGaIn. [9] Besides, EGaIn acts as an elastic material under pressure, and keeps its structural stability. [10] The desirable features of EGaIn make it popular for many applications like in the examples of a microstrip patch antenna [8], microstrip open state resonator [11], microfluidic implant coil for flexible telemetry system [12], a soft multi-axis force sensor using embedded microfluidic channels [13] and many others. All of these studies made use of the unique properties of EGaIn in an efficient way. However, oxidation leaves these properties in the shade when EGaIn is exposed to air. [1] Because of the gallium ingredient, EGaIn easily forms an oxide skin with exposure the air, and causes obstacles in many projects as a result, especially in the ones requiring a microchannel passage.

In this thesis, EGaIn has been chosen to employ as a liquid metal alloy considering the advantages over other LMs. It carries lower toxicity. It shows the characteristics of an elastic material until it experiences a critical surface stress, at which point it yields and flows readily. [10] Its high electrical conductivity and its tendency to make low contact resistance interfaces with a variety of materials makes EGaIn useful

for micro devices [14] This study requires the usage of micro channels, and EGaIn fills micro channels when sufficient pressure is applied. Moreover, it does not damage the structural stability in the channels when the proper amount of pressure is reached [10] In spite of all the benefits EGaIn has some drawbacks, too. The biggest problem with it is the generation of an oxide layer on the surface as mentioned above. Oxidation of EGaIn causes adherence to surface and thus hinders the movement of EGaIn plug.

There are some conventional methods headed for handling this problem although they have not turned out to be effective. Firstly, some studies have tried to use HCl strong acid by means of acid bath [15, 16] or vapor treatment [17]. Although these studies proved that HCl is effective in eliminating and preventing residues caused by oxidation of LM, using HCl is not convenient for many applications because of the strong acid. The second method, which has been tried to solve the oxidation problem, is using devices in a glove box. [4] Oxidation has not been observed in glove box experiments due to 0.001 ppm O₂ level inside the glove box. [4] However, it is a hard task to combine all the components of your study in a glove box, and this makes the method impracticable for many applications. The third method, encountered in the literature, is to fabricate lyophobic polymer surfaces. [18] When the contacting area of the channel surface gets narrower, the LM will actuate better. Even if this method seems successful, we cannot say that it has found the solution looked for, as it is not easy to adapt it to the other surfaces than the polymer one.

In this thesis, we will discuss how to handle this oxidation issue in microchannels to use the liquid metal plug as a normal liquid and to show that this experiment is

applicable for some RF devices mainly for tuning. Our methods and experiments will be explained in detail in the following chapters.

1.3 Conventional Liquid Metal Actuation

Liquid metal actuation has been the key challenge in recent studies trying to develop devices benefiting the unique properties of liquid metals. Liquid metal can be defined as an element or metal alloy in liquid phase at room temperature. In the past years, Mercury was the center of interest in a wide range of fields or applications from electrical devices to agriculture and pharmaceutical applications. It owes this popularity to being a liquid at room temperature and having a high conductivity inherently. However, due to having high toxicity and high vapor pressure, the products that contain mercury is limited or prohibited these days.

Conventional studies can be categorized into three groups in a general frame. These groups are the studies employing encapsulation of LM, pressure driven LM, and the droplet of LM. In the studies of encapsulating LM with an elastomer, they have achieved to make stretchable devices. They have been successful in making tunable devices by devising flexibility and stretchability of both liquid metal and elastomers such as PDMS and Ecoflex. In the pressure driven LM and droplet usage, the studies have required actuation of LM and they have tried to realize an effective actuation.

Khan et al dictated pressure to flow the LM in their microfluidic resonator design.[11] The oxidation issue was rather a benefit for them then a problem as it provided stability for LM. In the study of Kondoh and his colleagues, gas expansion was employed to move the liquid metal. [19] Their micromachined switch design will be

helpful to apply LM actuation in the other designs that can use gas expansion. Kim et al, on the other hand, used a different method and they implemented an electrostatic actuation. [3] In their study the LM droplet was driven by a given voltage bias that induces an electrostatic force between a grounded LM and an embedded actuation electrode. However, they could not find a solution to adherence problem, which requires too high driving voltage. Cumby et al used Laplace pressure for actuation of LM and they stated that the weakest link would be the liquid metal and oxidation if their device fabrication had been optimized. [20]

In a few more recent studies [21] [22], Teflon[®] solution was used as a coating material to alleviate the adhesion of LM to channel walls. They had success in eliminating the adherence to some extent. Nevertheless, they still suffer some problems as a result of optimization of the solution and its effect on the device like causing extra insertion loss.

1.4 Application of Liquid Metals in RF Components

Liquid metals have found a great area of applications such as thermometers, 3D electrodes and liquid mirror telescopes. Recently, RF components have been involved in these applications. The most prominent ones include switches [3, 23], inductors [24-27], antennas [7, 8, 28], resonators [11], filters [21], conductors [9, 29] and sensors [23, 30]. Many advances have been reached through the studies in these applications. Once the problems like oxidation are handled, LM is expected to bring much more improvements in science and technology especially with microfluidic RF components.

One of the most effective features of LM is the ability to adjust metal traces for

RF devices as tuning. [31] We will benefit this feature to fabricate a tunable inductor with a wide range of tuning via an on/off switching mechanism. Tunable inductors seem to be inseparable components in future measuring equipment and portable communication systems. They play a crucial role in various RF applications such as voltage-controlled-oscillators, tunable filters and antennas, and adaptive impedance matching circuits. [32] In fact, this component greatly affects the performance of transceivers and receivers. [24] Furthermore, it is promising for future works as MEMS technology is capable of realizing inductors with High-Q and large value. On chip implementation of these inductors are believed to be possible with technological improvements of our day, and this can lead to quite flexible systems.

A tunable inductor can be helpful in many RF circuits [33] and can be utilized in the designs of components and systems to acquire new compatibility and improved electrical performance over a wide range and frequency, smaller sizes, lower power consumption and less weight. [26] For instance, a tunable inductor can optimize the performance of RF circuits. [24] So, it is significant to develop the low loss variable passive components. [32] Unluckily, most of tunable inductors developed are lacking a high tuning range. [33]

Gmati et al proposed an RF MEMS tunable inductor with fluidic actuation using salt water to modify the capacitive coupling between metal spires and they achieved a wide tuning range [26] Chang and Sivoththaman presented an inductor with the thermal actuation of an a-Si and aluminum bimorph layer on Si at low temperature. They got high inductance values and a large tuning range at the end of their study. [25] In another

study, a tunable inductor consisting of a shielding metal plate and a MEMS actuator was developed. This inductor shifts the inductance by moving the metal plate above the spiral inductor. [34] Similarly to our study, Abidine and his colleagues made use of bimorph switches and the overall inductance changed with an on/off configuration. With this method, they acquired a good range without a continuous tunability. [24] Our study differs from this one in that we will use LM instead of thermal actuators and design the inductor on both PCB board and glass slides instead of a gold plate. Our design will be explained in a detailed way in the third chapter.

2. LIQUID METAL ACTUATION IN MICROFLUIDIC CHANNELS

Liquid metal actuation has become the subject of various studies. It has been a hard task to apply a perfect actuation in the microchannels, because the oxide skin that is readily formed with exposure to the air due to the gallium ingredient causes adherence to the channel walls and hinders the passage.

Xu et al. (2012) analyzed the effect of oxidation on the favorable features of EGaIn. They handled the issue with the method of acid bath in different concentrations and showed that it both prevented oxidation and helped to remove an oxide layer. [15] In the same way, Wang et al (2013) employed hydrochloric acid to dissolve the oxide layer locally in their study of reconfigurable liquid metal-based terahertz metamaterials. [16] However, direct contact with HCl causes limitations in many applications according the materials used. Kim et al showed that HCl vapor treatment could be used instead of acid bath. [17] Thus, an oxide free platform can be available for liquid metal. [35] Nevertheless, once the LM gets its static state will soon form on the surface although this gallium based oxide layer can be obviated with some external interventions. [36]

We felt urged to find a permanent solution, which is applicable for almost all substances unlike the acid bath confining the studies to the usage of certain materials. In following this goal of ours, experiments have been conducted on coating the channel walls and usage of some carrier liquids under different conditions and in both straight and loop channels.

2.1 Actuation of Liquid Metal in Straight Channel

The purpose of this paper in brief is to analyze the actuation of EGaIn in microchannels. Regarding the practicability arising from easy fabrication, stable sizes and even surfaces, straight microfluidic channels have been decided to employ in the analysis of LM actuation. The other reason to use straight channels is the fact that this usage means eliminating directly the undesirable extra factors such as a curve in the channel or change in the shape of liquid metal that affect the actuation in a negative way. In addition to these advantages, taking up a less space as a result of fabrication of in a row makes them preferable.

2.1.1 Design and Fabrication

To observe the actuation of liquid metal, a 3D master mold (LS 600, EnvisionTEC Inc.) that has straight channels has been designed by SolidWorks 3D CAD program. The channel dimensions have been defined as $50\text{mm} \times 2\text{mm} \times 1\text{mm}$ ($l \times w \times h$). After composing the design, the 3D master mold has been printed using stereolithography technique via 3D printer (ULTRA®, EnvisionTEC Inc., Dearborn, MI). Following the master mold process, an inverted replica of PDMS (Sylgard 184, Dow Corning, Midland, MI) channel has been made with soft lithography technique. Having peeled off the PDMS from the master mold, inlet and outlet holes have been punched at the ends of the channels using 1.5 mm biopsy punch (Acuderm Inc., Ft. Lauderdale, FL). By the same time we have spin coated the uncured PDMS on polymethyl methacrylate (PMMA) substrate at 2000 rpm for 40 sec, and cured it in $65\text{ }^\circ\text{C}$ oven for 3 hours. Then, the inverted PDMS layer of micro channel has been bonded to

the PDMS spin coated PMMA sheet via using O₂ plasma (100 um thick from spin-coating at 3000 rpm for 30 sec). The device and fabrication steps are shown in Figure 1.

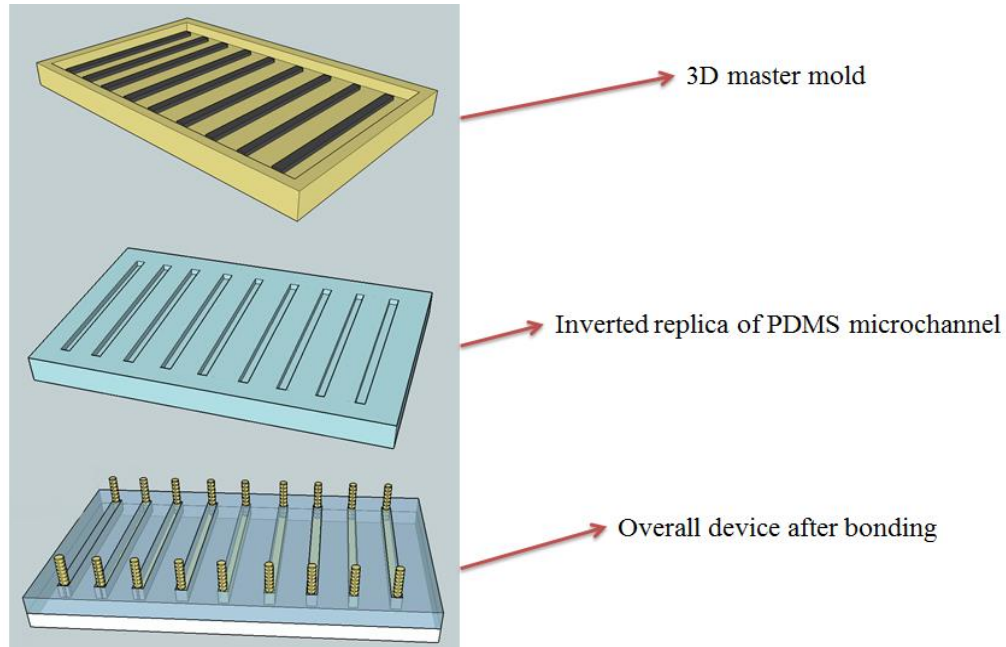


Figure 1: 3D Straight Channel Master Mold, Inverted Replica of PDMS and Whole Device

EGaIn instantly oxidizes and forms a skin around itself when it is exposed to oxygen (contacts with air) since it is a gallium based liquid metal. The skin tends to adhere to almost any surface. To handle this adhesion issue, we need to coat the channel to reduce the friction on the surface.

2.1.2 Effective Microchannel Coating

Our first approach for initiating the LM actuation test is to analyze the residue left inside the channel. Having fabricated the straight channels, we filled them with four different liquids as coating materials to observe the coating effect. These liquids are

Novec™ 2702 (3M, St. Paul, MN), 2% Pluronic® F108NF (BASF, Florham Park, NJ), 2% Tween® 20 (Sigma, Saint Louis, MO) and 5% PTFE (Sigma-Aldrich, Saint Louis, MO). The liquid metal plug with carrier liquid is inserted into the channels after N₂ gas has been blown to see whether LM skin formed by oxidation is sticking on the surface of the channel or not. We have prepared a table of channel pictures comparing the stickiness of skin layer of EGaIn plug with coating materials after LM has passed through the channels.

In selecting what to investigate as a coating material, we have conducted a research and used the past studies as a basis. Novec™ 2702 is a hydrophobic material and has an area of utilization in protection of PCB circuits from corrosion. [37] Pluronic® F108NF is known to be widely used for protein resistant coating onto PDMS surface to minimize protein adhesion. [38, 39] Tween® 20 is, likewise, used to prevent protein adsorption for PDMS channels. PTFE is generally used for non-stick coating for many applications in various areas.

We have tested the coating materials with seven different carrier liquids. The carrier liquids are DI water, mineral oil, mixture of mineral oil and 5% Novec™ 4300, Hydrocal®, mixture of Hydrocal® and 5% Novec™ 4300, Abil® EM 90 and Aquasonic® 100 Ultrasound Transmission Gel. The reason why we have chosen DI water to use is the fact that it is the easiest one to use as a carrier liquid. However, mineral oil has been chosen as an alternative, since water causes high loss at RF frequencies. [40] Hydrocal®, on the other hand, have been decided to add to the list as a result of having higher viscosity (442.44 cSt at 40°C) than that of mineral oil (viscosity: 15.3 cP at 40°C).

Novec™ 4300 has been tested, because it is a well-known surfactant in electronic processing. [41] Abil® EM 90 is a non-ionic emulsifier which is based on silicone, and thus, it has been determined as the other carrier liquid to be tested. What has made the Aquasonic® 100 Ultrasound Transmission Gel an alternative is the high viscosity it has. After all, 35 combinations of coating materials and carrier liquids have been tested.

Carrier liquid / Coating material	Water	Mineral oil	Mineral oil + 5% Novec 4300	Hydrocal	Hydrocal + 5% Novec 4300	Abil EM 90	Ultrasound Gel
No Coating							
Novec 2702							
2% Pluronic							
2% Tween 20							
5% PTFE							

Table 2: Images of Sticking Residue on Channel Surfaces after LM Actuation

As we can understand from the Table 2, in 5% PTFE coated channels, LM skin is not sticking on the channels and the channels keep the surface clean regardless of the surfactants, while most of the other channels coated with other materials seem darky due to stacked residues.

Besides; Novec™ 2703 coated channel with 5% Novec™ 4300 mixed with mineral oil, %2 Pluronic® F108NF coated channel with Aquasonic® 100 Ultrasound Transmission Gel, 2% Tween® 20 coated channels with surfactants such as 5% Novec™ 4300 mixed mineral oil, Hydrocal® and Aquasonic® 100 Ultrasound Transmission Gel have not posed sticking problem. These options can also be considered. However, when we employ the 5% PTFE as a coating material, we have observed no sticking on the surfaces of microfluidic channels. On the other hand, a sticking residue or skin in different amounts has been observed on the surfaces of the channels apart from the above-mentioned ones. Moreover, a great deal of residue has been observed in non-coated channels whichever surfactant has been used. This experiment proves the efficiency of the PTFE as a coating material. According to these results, it is understood that PTFE coating will help us in further experiments.

After deciding the coating material as PTFE, optimization of channel roughness has been tested by using different percentages of PTFE. For the experiments, 5%, 10%, 20%, 40% and 60% PTFE have been used. While testing different percentages of PTFE, at the same time, thermo treatment effects on PDMS microchannel has been investigated by heating the device at 200°C for 30 min after it has been filled with different percentages of PTFE and N₂ gas has been blown into it. (Table 3)











	5% PTFE coated channel	10% PTFE coated channel	20% PTFE coated channel	40% PTFE coated channel	60% PTFE coated channel
Not heated					
Heated at 200 C° for 30 min.					

Table 3: Different Percentages of PTFE and Thermo-Treatment Effects on PDMS Channel Roughness

For the experiments we are planning to conduct, we have printed out a 3D master mold by stereolithography technique at the first step. Secondly, we have made the inverted replica of the design using PDMS soft lithography technique. And thirdly, we have bonded the PDMS with glass with the O₂ plasma usage.

From the experiment, it is understood that the channel has been coated more with PTFE when the coating percentage increases, thus, thicker PTFE walls has been observed on the surface. This thicker coating is desirable for liquid metal actuation, but the switching pads will be affected by this coating if the LM actuates for switching. Thermo treatment effect on PTFE coated PDMS channel has been investigated, too. When the channel has been thermo treated at 200 °C for 30 min, the surface of the channel is smoother than the not heated channels. From all these experiments, it is easy to say that 5% PTFE coated and heated channel is good for acquiring sufficient coating and a smooth surface.

2.1.3 Effective Surfactant for Liquid Metal Carriage

In this section, our aim is to find the best surfactant, the carrier liquid in other words, for moving the liquid metal without leaving any residues. We have tested different surfactants with different viscosity rates to drive EGaIn in the microchannels. These surfactants are as follows; Hydrocal[®], mineral oil, Abil[®] EM 90, Span[®] 80, Aquasonic[®] 100 Ultrasound Transmission Gel and 30% PTFE dispersed in water.

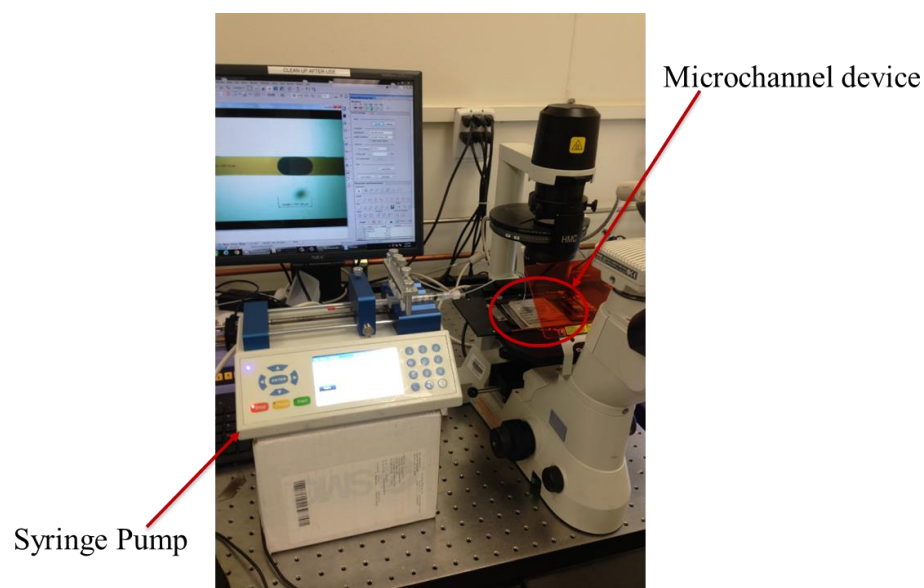


Figure 2: The Setup for Surfactant Test Analysis

The setup for surfactant tests is shown in Figure 2. The device has been tested using Fusion Touch 400 syringe pump (Chemyx Inc., Stafford, TX), Nikon Eclipse TS100 microscope (Nikon Inc., Melville, NY) and 3ml syringe (BD Inc., Franklin Lakes, NJ) with 15201 1/16 inch FEP tubing (IDEX, Oak Harbor, WA).
















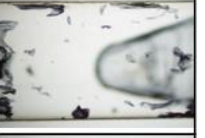








Surfactants	Initial State	After 1 st Run	After 3 rd Run	After 5 th Run
Hydrocal				
Mineral Oil				
Abil EM 90				
Span 80				
Ultrasound Gel				
30% PTFE				

Table 4: Left Residue Inside the Microfluidic Channels after LM Actuation 1st, 3rd and 5th Times Respectively

Residues left in the channel will not pose a big problem for switching just a few times even though it will affect the switching performance. Nonetheless, when you plan to do switching more frequently a perfect surfactant is required to clear away the residues. As one can comprehend from Table 4, most of the surfactants we tested gave us negative results with residue making at the end, but 30 % PTFE turned out to leave almost no residue.

PTFE powder is a good material for switching due to the low dielectric constant ($\epsilon_r = 2.1$). However, if the PTFE is diluted with DI water, the dielectric constant will increase in accordance with the dilution rate. More dilution will give us higher dielectric constant or higher conductance. Therefore, higher percentage of PTFE means better switching or RF experiments. PTFE is normally commercially available as 60% diluted in water (Sigma Aldrich Inc.). For liquid metal actuation, the viscosity of the liquid decreases when the dilution rate increases or the percentage of the PTFE decreases, and this causes uneven or non-smooth LM actuations. Although there are some positive factors that make us consider to choose 60% PTFE as a surfactant, there are also some drawbacks to take into account. The effect of evaporation of the water in diluted PTFE is observed more clearly in higher concentrations of PTFE. When the water evaporates, PTFE returns to its powdered or solid form. Thus, a clogging problem arises in microfluidic PDMS channels, generally in the inlet and outlet parts. 30% PTFE has been determined as the carrier liquid as a result.

For the following steps of the experiments, the relationship between the sizes of channels and LM plug will be analyzed.

2.1.4 Optimizing Channel Dimensions and Liquid Metal Sizes

Optimizing the sizes of the channels and LM plug is of vital importance to reflect the correct results of experiments. Here, we will try to find the most convenient channel sizes and LM sizes for the best movement of EGaIn and not leaving any residues. We've conducted a few experiments for actuation of liquid metal in straight channels.

According to the results of these tests, it is proved that there is a correlation between LM plug size and channel width and height ratio, which affects the liquid metal movement.

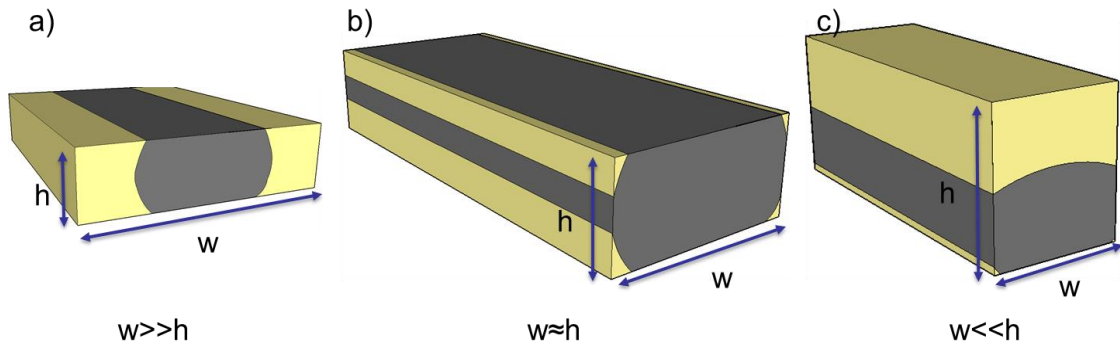


Figure 3: Liquid Metal in Different Channel Dimensions

In Figure 3, the different ratios of channel dimension and the position of liquid metal has been presented. When the channel width and height ratio is higher than a certain point, the liquid metal will stick in the middle of the channel while the carrier liquid flows through its sides. When the ratio is smaller than a certain point, this time the liquid metal will stay at the bottom of the channel with the impact of density, and the carrier liquid will pass above the liquid metal plug. If the channel width and height measurements are close to each other, this time the liquid metal can cover nearly all the cross sectional area excluding the corner region. In this experiment, we have focused on finding the best channel ratio to move the liquid metal plug efficiently. The density of the EGaIn is 6.25g/cm^3 , which is higher than that of water based carrier liquid.

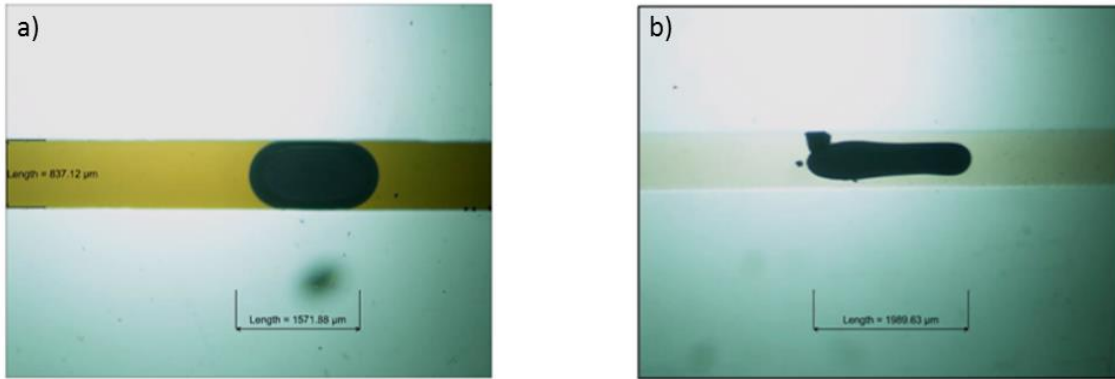


Figure 4: Images of EGaIn Plug in Different Channel (w/h) Ratios a) View of EGaIn Plug in the Channel Whose w/h Ratio Is 2, b) View of EGaIn Plug in the Channel Whose w/h Ratio Is 8

As seen in Figure 4a, the LM touches the walls and actuates well when the channel width and height ratio is 2. However, in Figure 4b, when the channel ratio is 8, the LM does not touch to the sidewalls, and 30% PTFE passes by the liquid metal plug without moving it as a result.

For this testing, a 3D master mold (HTM140, EnvisionTEC Inc., Dearborn, MI) for different ratios of straight channel has been fabricated using a 3D printer (MINI®, EnvisionTEC Inc., Dearborn, MI) to get a better resolution. While keeping the channel width as 500μm, height of the channels has been changed from 250μm to 2250μm to get 9 different channel ratios from 0.5 to 4.5. After cleaning and curing under UV light, the overall device has been fabricated with soft lithography technique and following the conventional techniques.

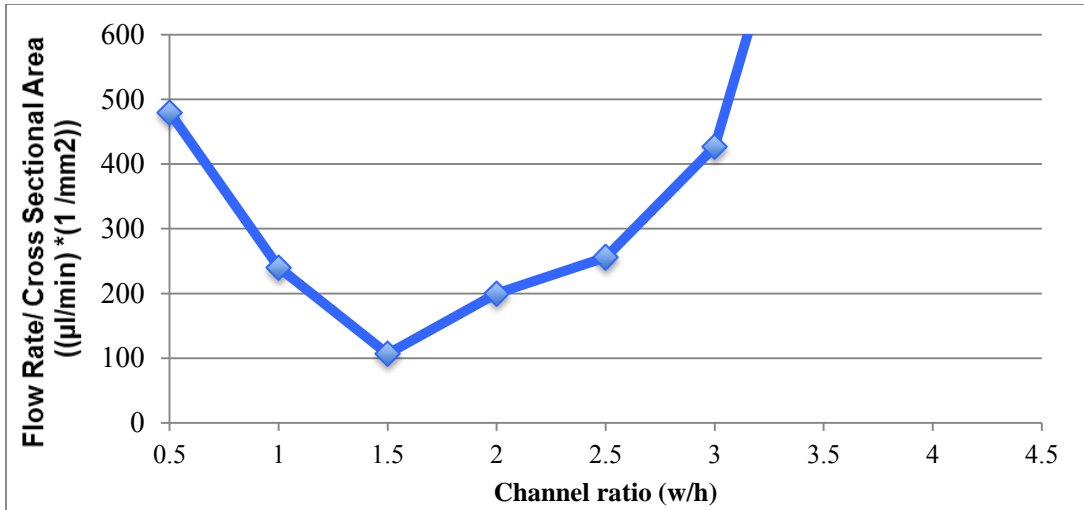


Figure 5: Minimum Required Flow Rate/ Cross Sectional Area to Channel Dimension Ratios

As we can interpret from the Figure 5, the required flow rate/ cross sectional area is minimum when the channel width and height ratio is around 1.5. If the channel ratio is below than 1.5, the liquid metal plug tends towards the bottom side of the channel, while a lower density of 30% PTFE is apt to pass over the plug. So, the carrier liquid will pass over the LM plug, and actuation will be slower and even stop in some point, and LM plug stays on the ground when the ratio is lower than 1.5.

Likewise, the carrier liquid passes by the plug from the sides while the plug stays in the midpoint of the channel if the channel ratio is over than 1.5. This causes discontinuity for LM actuation. When the channel ratio is over 3, no movement of LM plug has been observed, even if the flow rate inside the channels reaches $120\mu\text{l}/\text{min}$, which is the maximum channel flow rate that we can apply by syringe pump (Fusion

400, Chemyx Inc., Stafford, TX). Thus, in the following test, 1.5 has been chosen as the channel ratio to actuate LM plug in a straight channel.

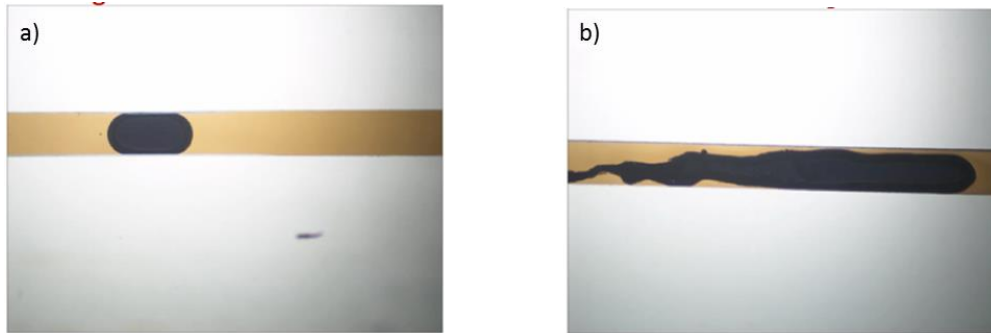


Figure 6: Images of Two Different Size EGaIn Plugs in the Same Channel (Width Is $500\mu\text{m}$) a) A Short Plug ($l/w: 2$), and b) A Long Plug ($l/w: 12$)

As it can be comprehended from Figure 6, we need to take the liquid metal plug size into consideration when we investigate the actuation of liquid metal in microfluidic channels. In Figure 6a, the liquid metal touches the walls and moves well while in Figure 6b liquid metal plug deforms and thus does not move since the liquid metal is too long even if the channel size is same with the one in Figure 6a.

If the plug length is smaller than the channel height or width, the movement of the liquid metal is not simultaneous with surfactant flow rate. Since the liquid metal does not touch the channel walls, it lets the carrier liquid pass by. For a better movement, LM plug size should be at least same as the width of the channel or the height of the channel whichever one is higher. If the LM plug size is longer than some certain ratio, liquid metal plug changes its shape, and the carrier liquid passes through the channel without moving the LM. (Figure 7a & 7b)

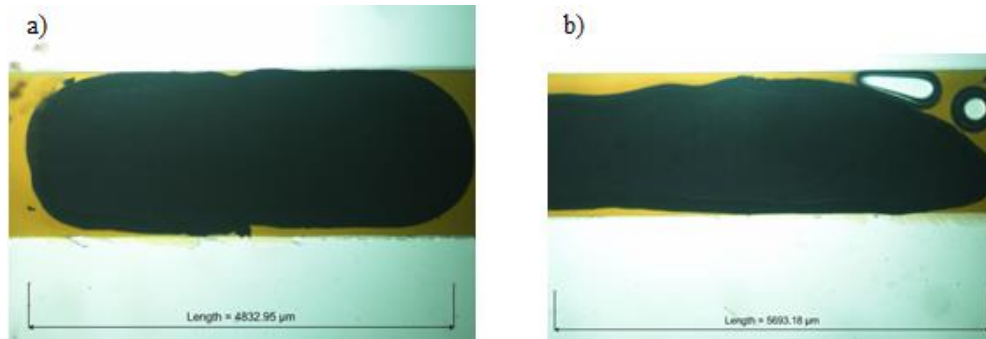


Figure 7: Images of EGeIn Plugs in Different Lengths in the Same Channel (Channel Width Is 2000 μm) a) The Plug Is Short Enough to Move, and b) The Plug Is Longer Than the Threshold Length

In this experiment, the ratio of liquid metal length to channel width has been investigated while fixing the channel dimension ratio to 1.5. We have tried to demonstrate how many times longer plug can be used for a given width of channel.

(Figure 8)

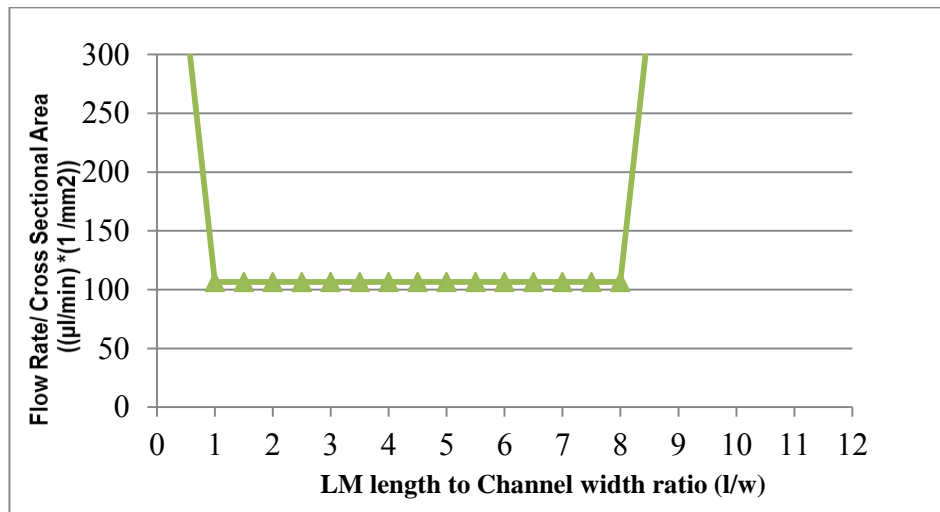


Figure 8: Effective Liquid Metal Length to Channel Width Ratio (Channel Width Is 500 μm). If the l/w Ratio Is Between 1 and 8, Flow Rate/Cross Sectional Area of Channel Is Minimum for Actuating Liquid Metal. In the l/w Ratio Other Than This Range, the Plug Does Not Move.

For the plug length optimization experiment, the width of the microfluidic channel has been determined as 500 μm and the channel width and height ratio (w/h) has been fixed to 1.5. At the end of the experiment, having tested the liquid metal in different lengths, it has been decided that l/w ratio of the microfluidic channel is fine from 1 to 8 to achieve a flawless movement. In other ratios than the abovementioned one, the shape of the liquid metal plug has been observed to deform. Thus, no movement of liquid metal plug has realized even the flow rate is as high as 1ml/min.

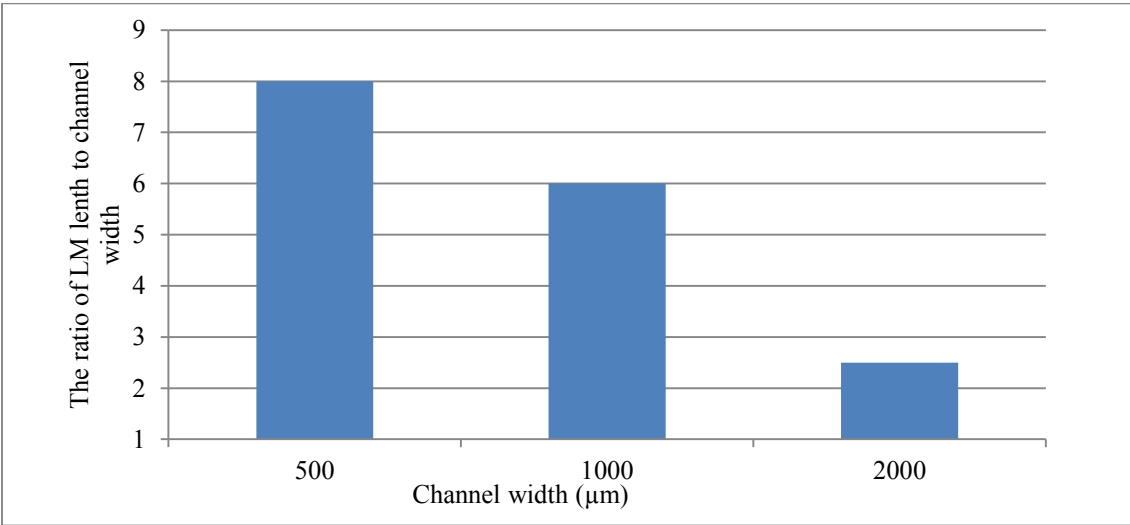


Figure 9: Effective L/W Ratio for Actuating Liquid Metal with Given Channel Widths as 500 μm , 1000 μm , and 2000 μm Respectively

In this experiment, under the light of previous experiment, the channel width to height ratio has been chosen as 1.5. As it is seen in Figure 9, when the channel width is nearly 500 μm , the liquid metal length to channel width ratio should be within the range

of 1 to 8, and this range becomes 1 to 6 for the channel that is nearly 1000 μm in size while it should be 1 to 2.5 for the channel with 2000 μm width to actuate the liquid metal plug without changing its shape. If the ratio of LM length to channel width is smaller than 1, the carrier liquid passes through both sides of microfluidic PDMS channel. When the range is bigger than their threshold ratio, the 30% PTFE squeezes the LM plug towards one side of the channel and passes through it. This experiment makes it clear that we should take care of the inserted liquid metal length in addition to the channel width and height ratio when we use LM plug inside the microfluidic channel with 30% PTFE.

2.2 Actuation of LM in Closed Loop Channel

2.2.1 Design and Fabrication

Up to now, we have tested the liquid metal actuation by using syringe pull and push pressure in straight channel to see the movement by minimizing the effect of other variables. This straight channel is good for the starting structure; however, another aim is to drive the LM itself without hand force and make a more reliable and continuous device for actuating liquid metal. Using lithography technique for a multi-layer structure allows us to make more complicated channel designs. For a more automated system without needing continuous syringe flow and human force, a three layer closed loop channel has been designed and fabricated. (Figure 10)

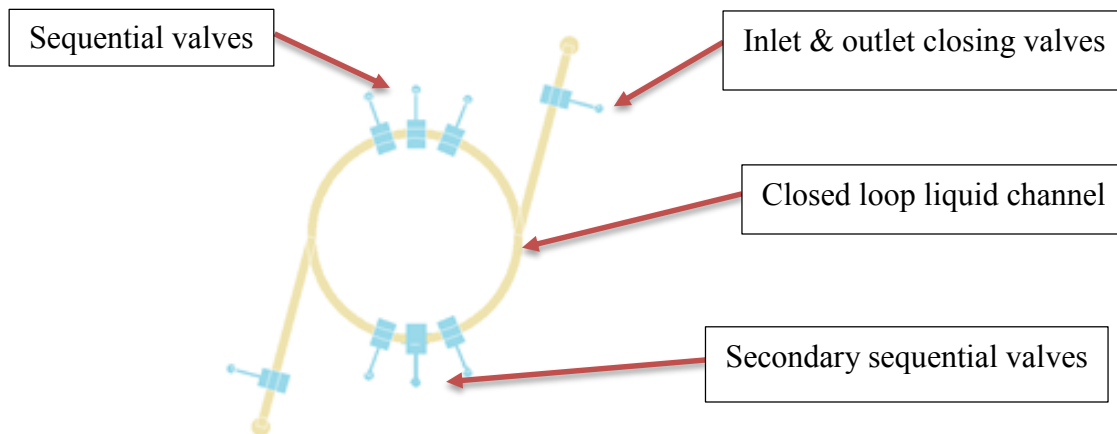


Figure 10: Overall Closed Loop Design

By the help of this device, LM can actuate with the pushing force of the microfluidic valves, which actuate with N_2 gas. The other advantage of this design is that the direction and speed of LM actuation can be adjustable using the sequential valves. With the help of the secondary peristaltic valves, the LM plug can be manipulated in both directions. To increase or decrease the speed of the liquid metal plug, the valves dimensions should be adjusted. The larger valves will give a faster speed.

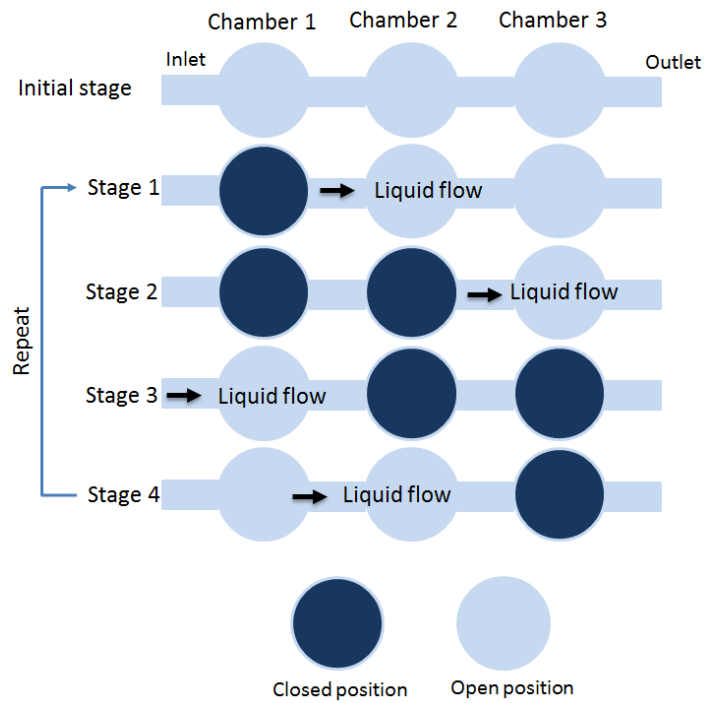


Figure 11: The Working Principle of Peristaltic Pump with Microvalves

Figure 11 demonstrates us the actuation mechanism of peristaltic pump. In the initial stage, all the chambers are in open position, and this means the flexible membrane between the control channel and liquid channel is flat. In stage 1, the chamber 1 is closed by the flexible membrane, which is suppressed by the injected N_2 gas, while the other two chambers remain in open position. Then the liquid flows through the open chambers in both directions. In stage 2, the second chamber closes and the liquid needs to move through the open chamber in a certain direction, since one direction is closed via the first chamber. If this process follows the sequence of Figure 11, the liquid will move in a certain direction with certain amount of liquid and speed. For this type of peristaltic pumping mechanism, at least three chambers are required.

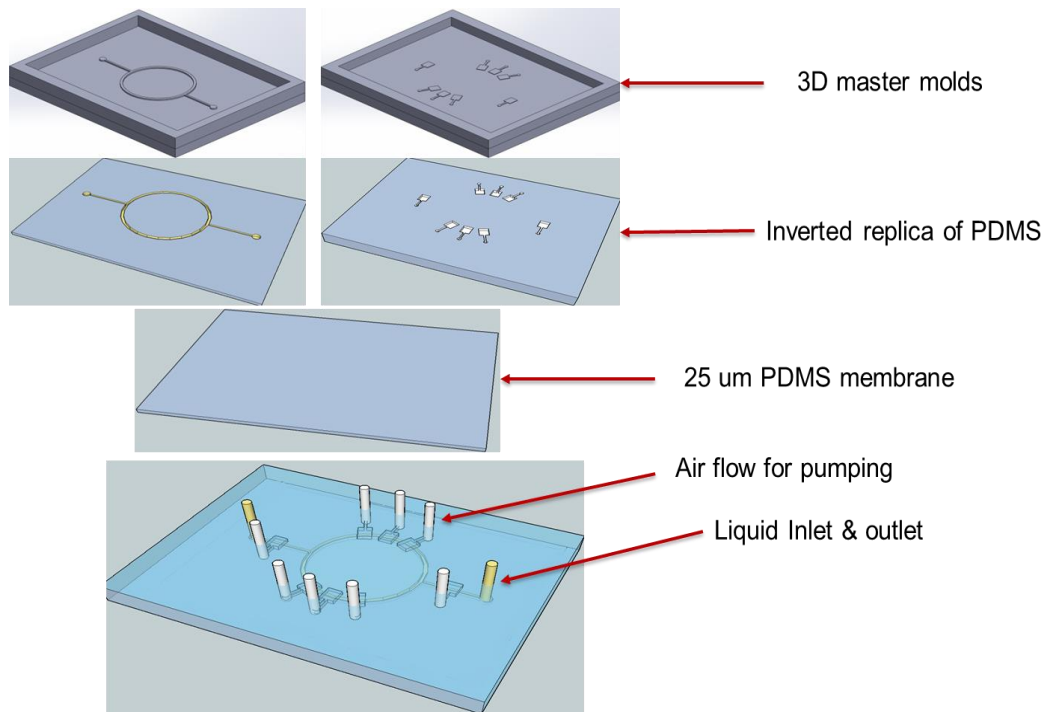


Figure 12: Fabrication Steps of Closed Loop Device

The fabrication steps of closed loop device are shown in Figure 12. By using the 3D printer (MINI®, EnvisionTEC Inc., Dearborn, MI), the master molds of both closed loop channel and control valves have been fabricated. With the help of the PDMS soft lithography technique, an inverted replica of the channel and pump layer have been fabricated. By applying O₂ plasma, after bonding the pumping layer with 25μm PDMS thin membrane which has been processed by 3000rpm spin coating PDMS on Si wafer, we have bonded the channel layer with the PDMS membrane which has been bonded before with pumping layer. Also 2 by 3 inch glass slide has been attached to the channel layer to keep the bottom layer of the device clean and stable. By doing so, we have obtained the closed loop channel with several micro valves.

2.2.2 Experimental Steps and Results

To handle the valves sequence and inlet and outlet valves, we have designed an interface in the software LabVIEW™, which we employ for controlling the solenoid valve mechanism. We have manipulated the N₂ gas airflow with the help of multi-channel peristaltic pump. Having filled the channel with the carrier liquid and inserted liquid metal plug into the channel, we have closed the inlet and outlet parts of the channel by valves. When the valves are filled with pressurized nitrogen gas, the membrane over the channel will move downward, and it will move the liquid under the valve in both directions. When the second valve is on, while the first one is still on, the liquid under the valve will be pushed through one direction. To give a directional movement of liquid, at least three valves in a sequence are required.

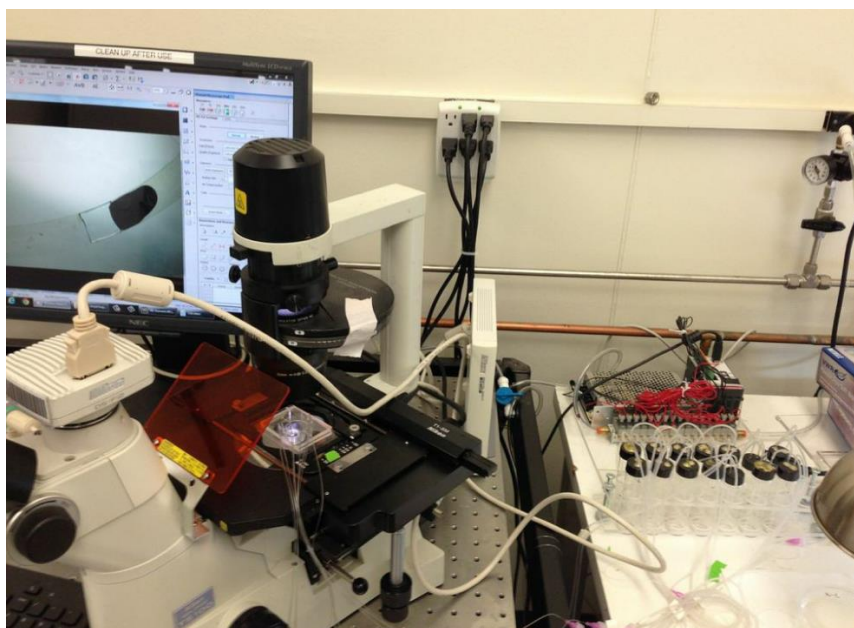


Figure 13: The Overall Setup for LM Actuation in Closed Loop Device with the Solenoid Valve Controller

The setup for closed loop device testing is shown in Figure 13. What have been employed in this study are the software LabVIEW™ and a solenoid valve controller with tubing to monitor the control valves. The solenoid valve controller has been connected to N₂ gas and vacuum pumps.

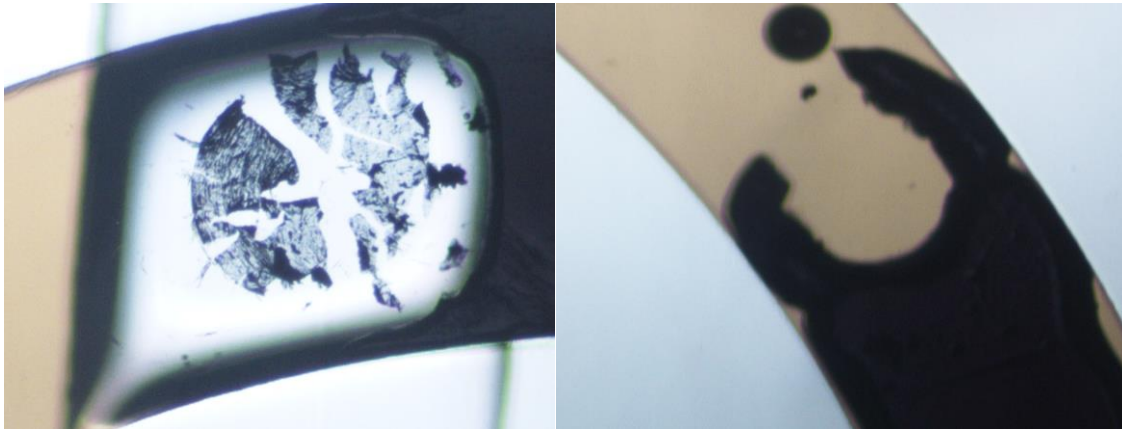


Figure 14: Images of EGaIn Plug under the Valves and after LM Passage

There exists one issue with using peristaltic pumping mechanism that the plug can be divided under the peristaltic pump when the liquid metal passes under the valves. (Figure 14) To prevent this problem, we have inserted the secondary peristaltic pump. In Figure 15a and 15b, the designs of closed loop channel with and without secondary pumping system is exhibited. While the liquid metal is passing under the first peristaltic pump, it will stop and the secondary peristaltic pump will move the liquid metal. Thus, the liquid metal plug can be moved in all closed loop. The only disadvantage of this system is that we have to adjust on/off position of each pump manually. However, if we

succeed in optimizing the movement of LM in a second, we can do this switching with LabVIEW™ as well.

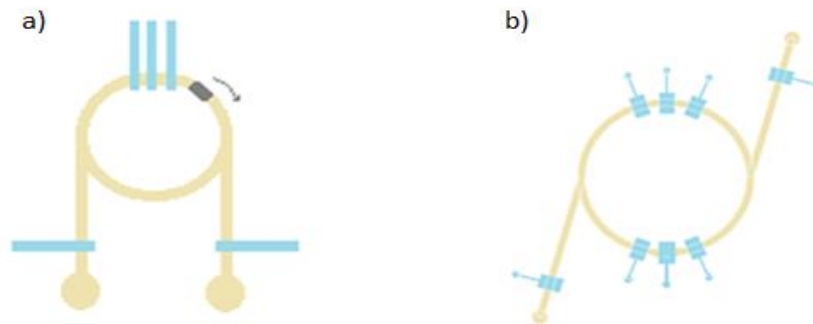


Figure 15: Designs of Different Closed Loop Devices a) Design with Only One Sequential Pumping, and b) Design with Secondary Sequential Pumping

The latter design with secondary sequential valves has solved the issue of LM division under the valves. When the liquid metal passes under one of the sequential valves, the secondary peristaltic pumps will push the LM plug.

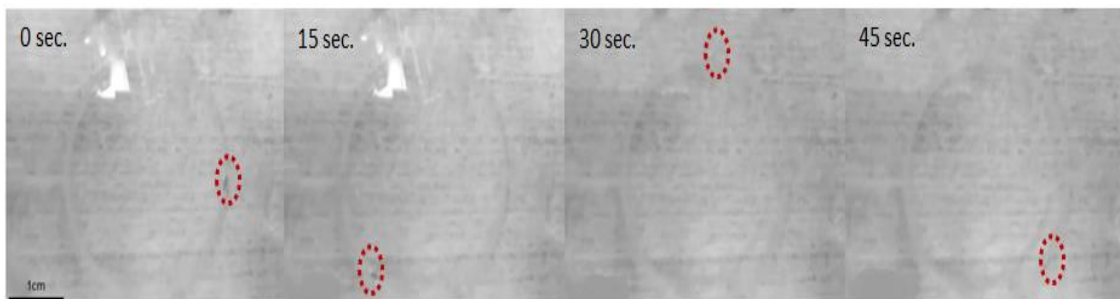


Figure 16: Images of LM Movement in Closed Loop Device with Respect to Time

As depicted in Figure 16, a clear actuation of Liquid Metal alloy, EGaIn, without any division or stickiness has been achieved. A complete movement around the closed loop chamber has taken up less than 45 sec. The average speed calculated during the movement has been 75.5mm/min. The actuation has been tested 10 cycles and the time for each turning is nearly the same. For future experiment, the repeatability and consistency will be our goal to get a stable movement. In addition to this the speed of the liquid metal plug has been calculated with different device from 7.5mm/min. to 75.5mm/min. 10 times higher speed has been achieved with changing the designs. Because the speed of the liquid metal is related with the valve size and device dimensions, the further experiment will be done to optimize the speed and consistency.

$$S_{21} \text{ (dB)} = \text{Forward Gain} = 20\log S_{21}$$

$$S_{12} \text{ (dB)} = \text{Reverse Gain} = 20\log S_{12}$$

The conversion of dB parameters for each gain is reflected in the equations above. While S_{21} in ON state, which means the liquid metal is on the transmission line pads; it will give us the forwarded gain. When it is in OFF state, there will be dielectric liquid instead of liquid metal in the switching region, and S_{21} will show us the transmitted loss.

After printing the inductor design on PCB, the uncured PDMS has been spin coated on the top of the PCB. The channel place has been cut by means of the laser machine after waiting overnight in the oven at 65 °C for curing. Then, the inverted replica of the channel PDMS layer, which has been prepared formerly with soft lithography technique, has been bonded with PDMS on the top of the PCB. Figure 18 shows the fabricated switching testing device.

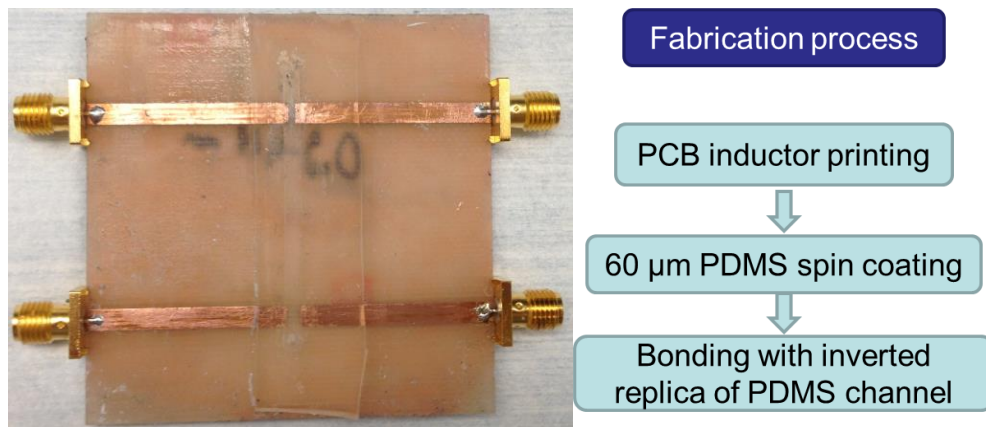


Figure 18: RF Switching Device and Fabrication Steps

For the experiment, we have tested the switching performance applying various surfactants. Hydrocal[®], Aquasonic[®] ultrasound gel, 5%, 10%, 20%, 30% and 60% PTFE solution have been tested as surfactants.

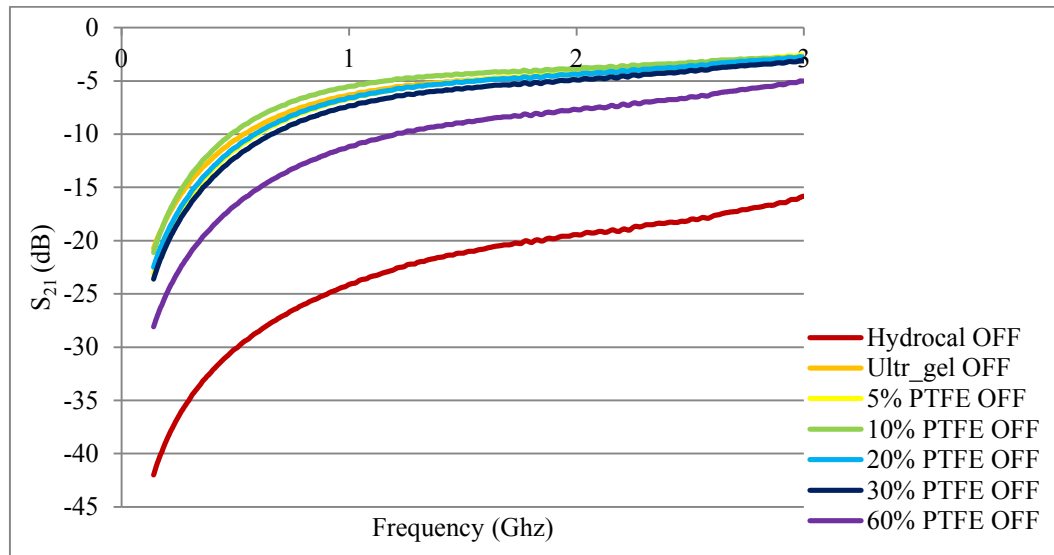


Figure 19: OFF State S_{21} Forwarded Gain of the RF Switch with Different Surfactants

This figure depicts the forwarded gain or transmitted signal via different surfactants and various percentages of some surfactants when the switch is in OFF state. (Figure 19) At 200 MHz, Hydrocal[®] shows only 1% signal transmission while 5.6% of the signal passes with 60% PTFE, and 10% of the signal passes with 30% PTFE. At 2 GHz, nearly 10%, 40%, 56% of the signal has been observed to be transmitted with the Hydrocal[®], 60 % PTFE and 30% PTFE, respectively. This fact clarifies that the Hydrocal[®] is a better dielectric than diluted PTFE at these frequencies.

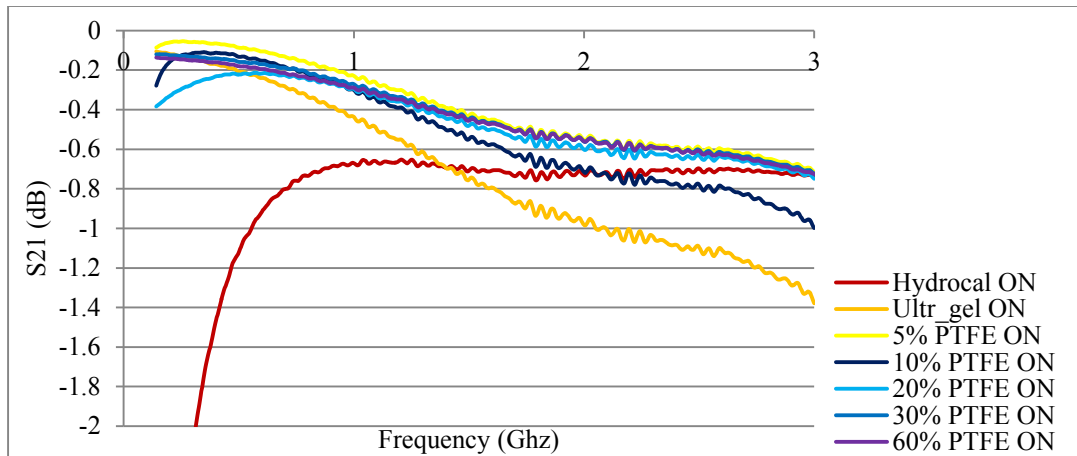


Figure 20: ON State S₂₁ Forwarded Gains of RF Switch with Different Surfactants

Forwarded gains of the switch with different carrier liquids are shown in Figure 20. As depicted in the figures, Hydrocal[®] is a better dielectric due to its dielectric constant, which is 2.35. Although the dielectric constant of the powder PTFE is as low as 1.9, when it is mixed with the deionized water whose dielectric constant is nearly 80, the diluted PTFE's dielectric constant will vary according to the dilution percentage.

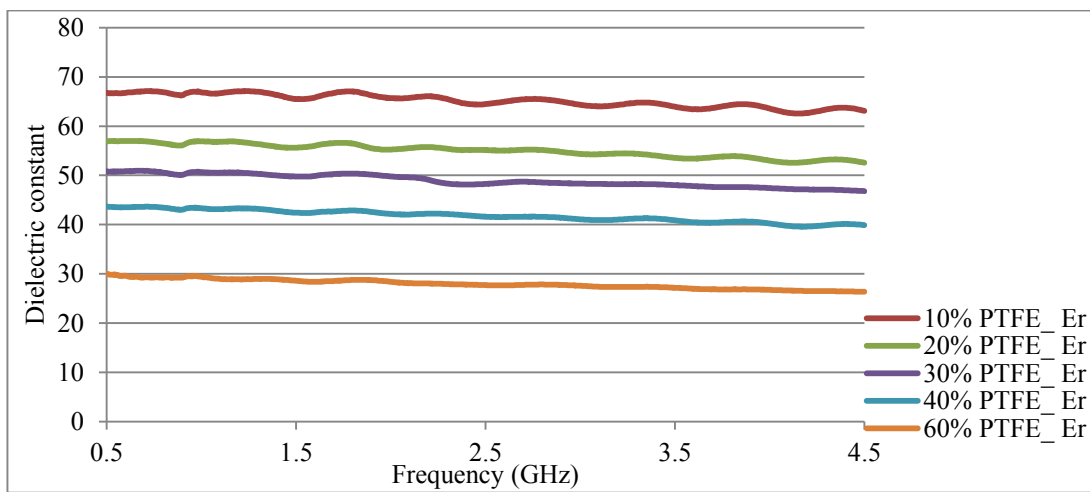


Figure 21: Dielectric Constants of Diluted PTFE Solutions

These results show the dielectric constant of different percentages of PTFE solutions. (Figure 21) As we have expected, the dielectric constant of PTFE ($\epsilon_r = 1.9$) increases as the dilution rate increases. For RF perspective, getting a carrier liquid with higher dielectric constant means more conductivity. In our experiment, when the liquid metal is ON state, which means that it is between the conductive pads of transmission line, the LM will act as a transmission line by passing the signals. In our design, while LM is used as a conductor, the carrier liquid is used to carry LM and it acts as a dielectric material. When the switch is in OFF state, the carrier liquid should reflect the signals back without transmitting as an ideal case. However, the liquid will transmit the signal partially if it is conductive or have a high dielectric constant. In our experiments, lower percentages of PTFE will not be an effective carrier liquid or dielectric material for our RF device.

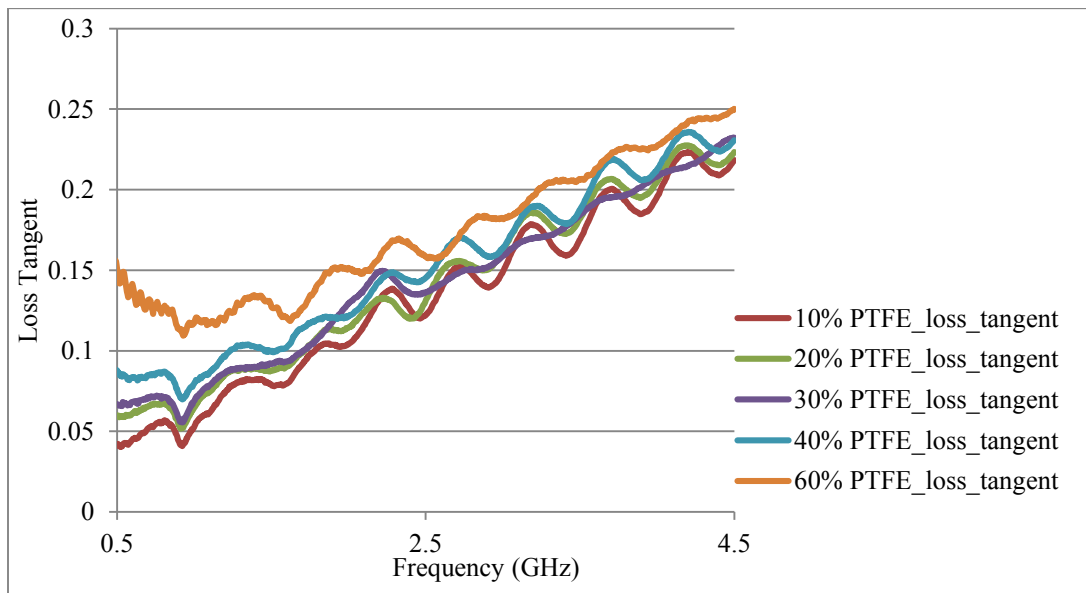


Figure 22: Loss Tangent of Different Percentages of PTFE Dilution

$$\text{Dielectric loss} = \frac{\sigma}{2} \sqrt{\frac{\mu_0}{\epsilon}}$$

In terms of the loss tangent, which shows the loss of the medium, the higher loss tangent means more dielectric loss. As it is seen in Figure 22, the higher concentration of PTFE solutions has higher loss tangent, and makes the surfactant imperfect. At 3 GHz, the loss tangent of 60% PTFE is nearly 0.18 while the loss tangent of 10% PTFE is nearly 0.16. However at 3 GHz, the dielectric constant of 60% PTFE is around 27.5 and 10% PTFE is around 64.4. If we calculate the dielectric loss of each, 10% PTFE seems nearly 1.36 times higher dielectric loss than 60% PTFE. If the result is compared to the switching experiment, at 3 GHz, S_{21} transmitted loss with the 60% PTFE is -5 dB means, %56 percent loss and while S_{21} with 10% PTFE is nearly -2.5dB means, %75 loss. It means that 10% PTFE nearly 1.35 times lossier than 60% PTFE as also calculated.

3.2 Design and Fabrication of Tunable Loop Inductor

The all fabrication steps of loop inductor design on glass substrate are shown in

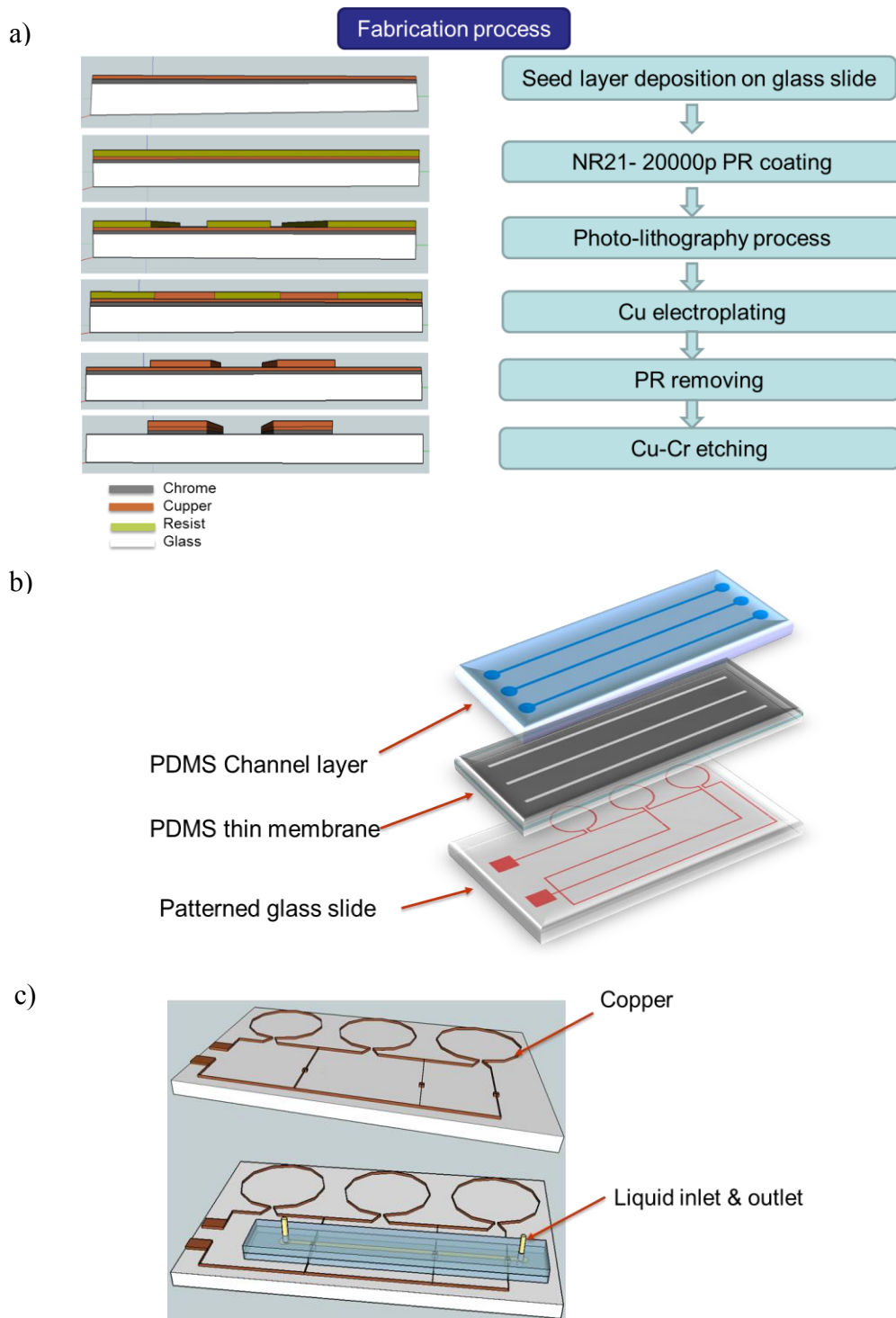


Figure 23: Tunable Loop Inductor Design a) Fabrication Process of the Inductor Patterned on a Glass Slide, b) Channel Layers, and c) Overall Device

Figure 23. Through the instrument of lithography technique, a loop inductor on a glass slide has been fabricated. In fabrication steps: Cr and Cu seed layers have been deposited on a glass slide that has been cleaned with Piranha solution, a mixture of sulfuric acid and hydrogen per oxide, in advance. Futurex[®] negative resist has been spin coated on the top of the glass and the photolithography process has been applied. The patterned glass slide has been put in Cu electroplating solution afterwards. The resist has been removed by using Acetone. The etching solution for Cu and Cr has been utilized to remove the seed layers. After all of these processes have been carried out, trichlorosilane coating has been used before spin coating PDMS on the device. Soft lithography technique has been implemented to make a PDMS channel on the top of it. Before bonding process we have taken out the channel layer of PDMS by means of laser machining. Therefore, our channel touches on the glass surface and forms a smooth surface for the channel.

In the Type 1 inductor design (Figure 24a), there are 3 channels, each of which is for one switching part. When the LM plug passes on the switching point of the first channel, only one inductor will be ON. If the liquid metal in the second channel passes on the switching part, two coils will be ON. If the LM plug in the third channel passes the switching part, three coils will be ON.

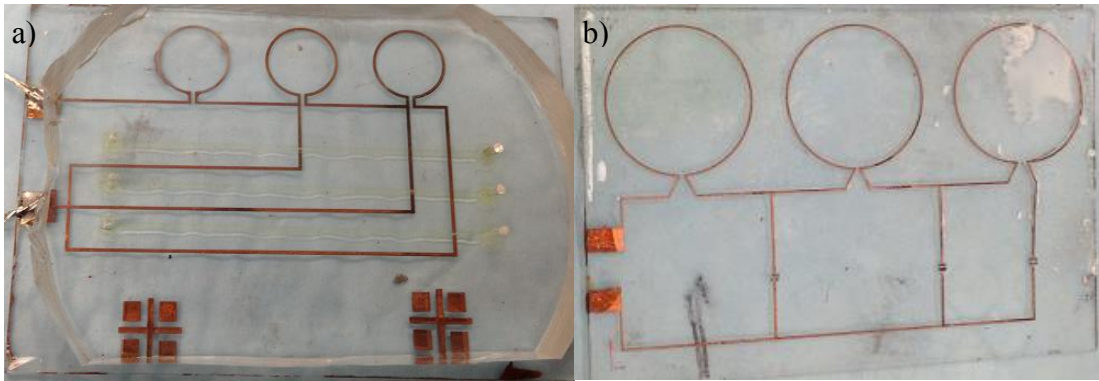


Figure 24: Two Different Inductor Designs a) Type 1 Tunable Inductor Design b) Type 2 Tunable Inductor Design

In the Type 2 inductor design (Figure 24b), there is only one channel that has three switching parts. When the LM plug passes on the first switching part, only one loop will be ON, when it passes the second and third switching parts, two and three loops will be ON, respectively.

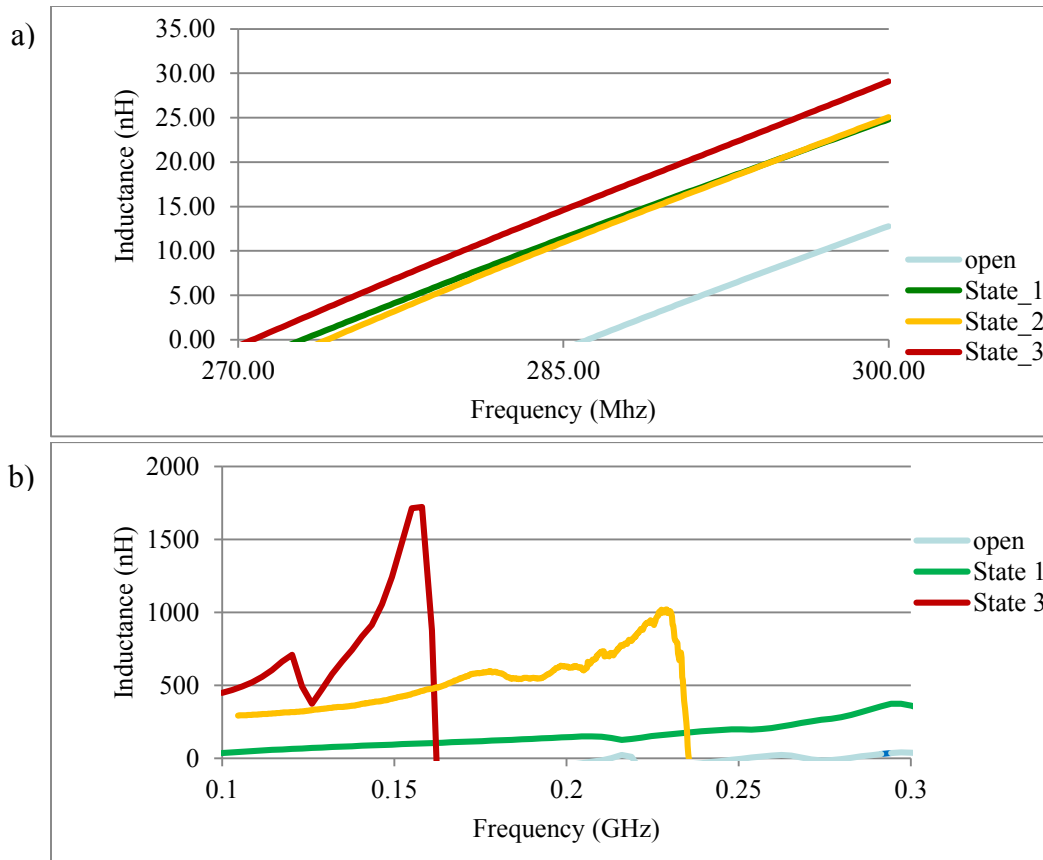


Figure 25: Inductance Result Graphics of Tunable Inductors a) Results of Type 1 Tunable Loop Inductor, and b) Results of Type 2 Tunable Loop Inductor

The aim in testing these devices is to show the inductance variation by using the switching mechanism of EGaIn. As one can see from Figure 25, the inductance increases as the number of inductive loops increases. At 1.56 GHz, an inductance change from 100 (nH) to 1700 (nH) has been observed. (Figure 25b) Therefore, a nearly 1600% tuning range has been reached.

These devices have been fabricated to analyze the tunability of inductor by microfluidic actuation of LM plug in PDMS channels. There are some crucial drawbacks of this design, which make it worthless for using in actual RF devices. One of the crucial

factors is the transmission line design. For actual RF devices, it requires 50Ω matching networks and 50Ω lossless transmission line designs. Another important factor that affects our results is the connection of the copper pads on glass to SMA connector. The high mutual inductance between the coils and transmission lines has also a place among crucial factors. To overcome these challenges and design a better tunable inductor, the inductor design on PCB will be explained in the following chapter.

3.3 Tunable Spiral Inductor on PCB

3.3.1 Spiral Inductor Design with Straight Channel

We have designed a tunable spiral inductor on FR4 based PCB. After designing and printing out the device, a similar process for making a PDMS channel for switching points has been performed. Straight channel PCB inductor has been designed and fabricated. (Figure 26)

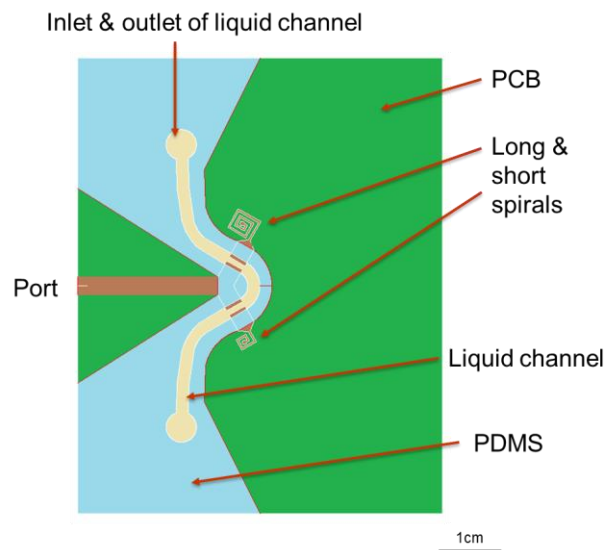


Figure 26: Illustration of the Overall Design of PCB Tunable Spiral Inductor with Straight Channel

On FR4 substrate PCB, two different spiral coils with nearly 3mm width of microstrip transmission line and 800 μ m switching gaps have been designed and simulated with the use of finite element method solver (HFSS). While the long spiral has 2.5 turns, the short coil has 1.5 turns.

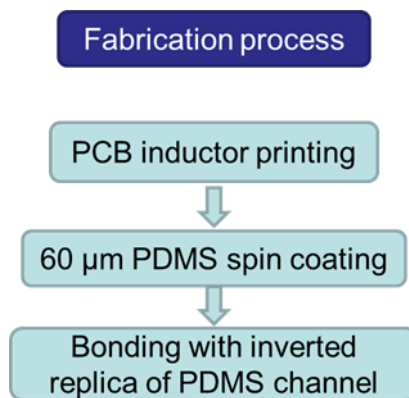


Figure 27: Fabrication Steps of PCB Inductor Design

Fabrication steps of PCB inductor are shown in Figure 27. As fabrication process, after printing PCB inductor, the PCB has been spin coated with PDMS at 2000 rpm at 40 sec. The thickness of the copper trace on the PCB is around 35 μ m, and thus the spin coated PDMS on PCB should be bigger than 35 μ m. After curing the PCB in 65 $^{\circ}$ C oven for 3 hours, it is bonded with the inverted replica of the microfluidic channel which has been punched before similarly to the former lithography technique.

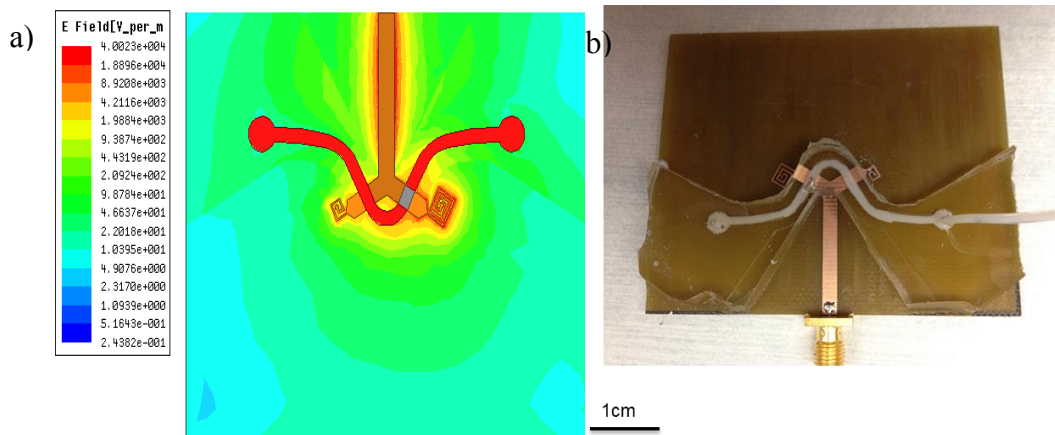


Figure 28: a) E-Field Distribution of Simulated PCB Inductor While Long Inductor Is ON b) Fabricated PCB Inductor Design with Straight Channel

E-field distribution of the PCB inductor design with straight channel has been simulated by using HFSS. In Figure 28, both the simulated E field distributions and the fabricated device are demonstrated.

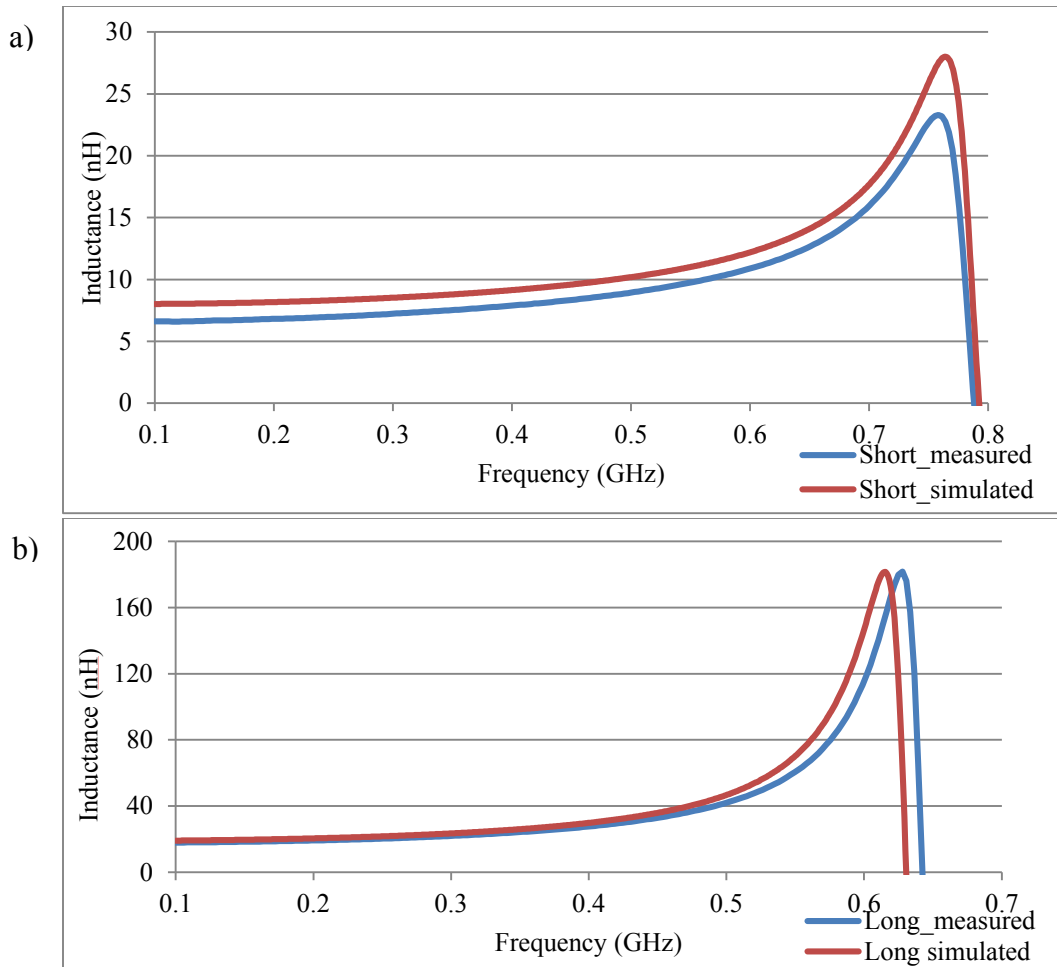


Figure 29: Simulated and Measured Results of Spiral Inductor a) Inductance of Simulated and Measured Short Inductor, and b) Inductance of Simulated and Measured Long Inductor

Comprehensible from Figure 29, the simulated and measured inductance nearly matches each other. Nevertheless, there are still some differences in the inductance. The reason behind these differences may be the case of the SMA connection with transmission line and/or the connection problem with LM plug and the transmission line pads. At 0.6 GHz, an inductance change from 12 (nH) to 180 (nH) and a tuning range of nearly 1400% have been achieved.

3.3.2 Spiral Inductor Design with Closed Loop Channel

We have also designed a closed loop device on the PCB inductor in accordance with our previous results. The effectiveness of this process is elimination of the need for continuous hand pull and push pressure due to micro pumps and controller to achieve actuation of LM plug with desired direction and speed.

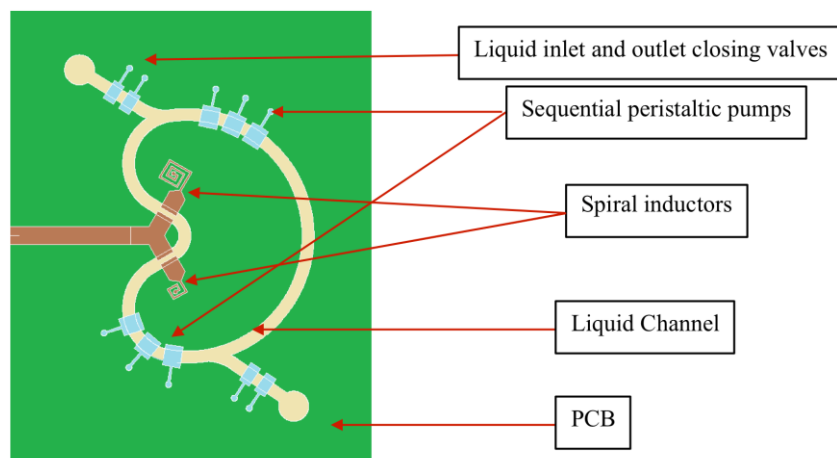


Figure 30: Illustration of PCB Inductor Design with Closed Loop Channel

The closed loop channel has also been designed on the top of PCB inductor in line with the aim of this project which is to devise a tunable RF inductor by actuating liquid metal with more automated systems. (Figure 30) With the help of solenoid valve controller, without need for the hand pull and push pressure; an automated LM plug actuation has been achieved on PCB inductor. The speed and movement of LM can be adjustable by changing the valve and channel sizes. Therefore, the effectiveness, repeatability and consistency of the device are expected to improve.

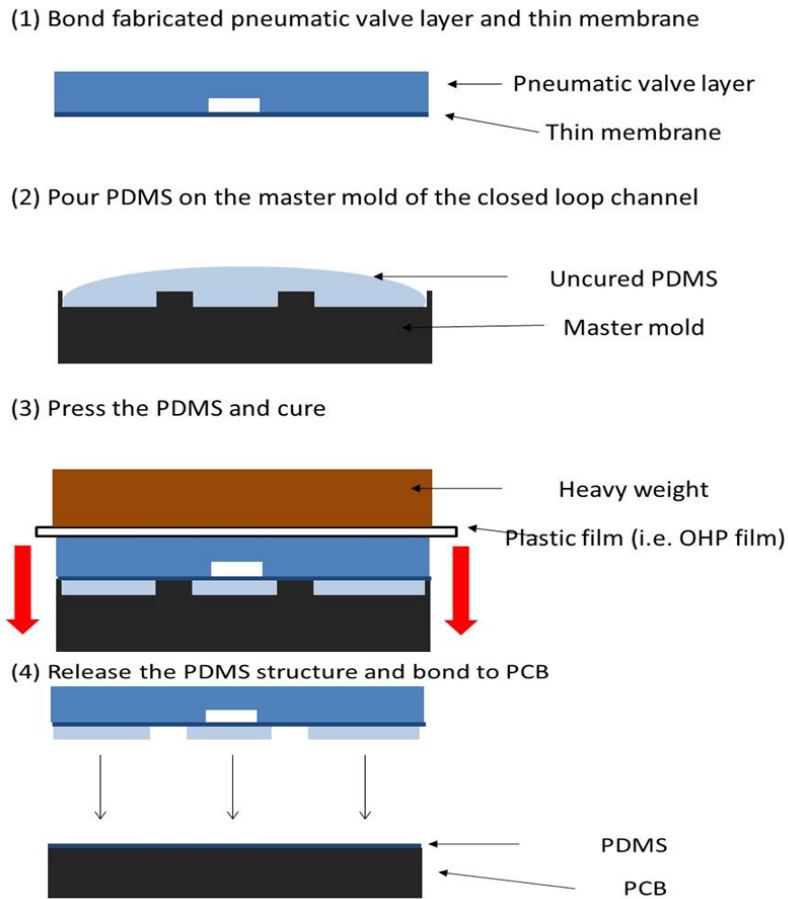


Figure 31: Fabrication Process of Closed Loop Device on PCB

The 3D master molds for valves and microfluidic channel has been fabricated at the first step of the device fabrication process. (Figure 31) The valve layer inverted replica of PDMS valve layer has been achieved by using soft lithography technique after cleaning the master mold, curing it under UV light, and coating the cured master mold with tridecafluoro-1,1,2,2-tetrahydrooctyl trichlorosilane. Peeling off and punching the valve holes of the PDMS valve layer have been followed by bonding with 25 μ m PDMS membrane, which has been spin coated at 3000rpm for 40 sec and with 2 hour 85 $^{\circ}$ C

curing. Afterwards, the uncured PDMS has been poured on the liquid channel master mold and degased for 10 min. In the next step, the bonded valve layer and membrane has been putted on the top of the uncured PDMS filled closed loop master mold by using plastic film and heavy weight on the top of the valve layer. After completion of aligning, it has been cured at 65°C in oven for 3 hours. Then, the valve layer bonded with membrane and cured with channel layer has been peeled off carefully. Finally, it has been bonded with 60µm PDMS coated PCB spin coated at 2000 rpm for 40 sec. The overall fabricated device is shown in Figure 32.

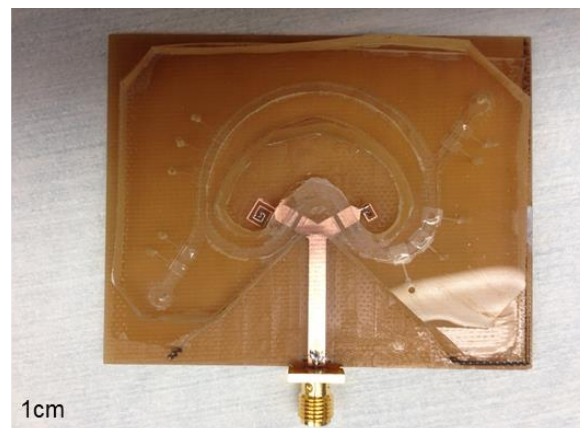


Figure 32: Fabricated Closed Loop Device

4. SUMMARY AND FUTURE WORK

4.1 Summary

The increasing interest and the great advancements in liquid metals is the driving force behind this thesis project. Once we are convinced that the significant properties of liquid metals can be combined with the lab on a chip technology and even with radio frequency components in the further step, this thesis study is initiated naturally.

Recognizing that there is a hindrance for the studies aiming at liquid metal actuation, which is the oxidation problem of gallium containing liquid metal alloys, our efforts has been directed to eliminate this problem. EGaIn has been determined as the liquid metal alloy to employ in this project. So as to analyze the actuation of EGaIn in microfluidic PDMS channels, different coating materials and carrier liquids have been tested at the first place. In total, 35 combinations of coating materials and carrier liquids have been tested at the end of the experiments. It has been observed that PTFE provides a clear actuation without any residues caused by the stickiness resulted from oxidation both as a coating material and a carrier liquid.

In the second phase, this actuation has been tried to exemplify in an RF inductor to demonstrate and investigate the effectiveness of conductive liquid metals in RF components. Tunability is the feature of our inductor enabled with the usage of EGaIn. As prototypes, two different tunable loop inductors have been designed on a glass slide. A spiral inductor has been designed on PCB to act as a tunable RF inductor, afterwards.

Measurements have been done and only a slight difference has been detected between the simulated results and the real ones.

At the end of the project, a solution to oxidation problem of liquid metals is offered, tunability is provided in an RF inductor using liquid metal as a switching part and lastly the feasibility of liquid metals to electrical device applications is introduced.

4.2 Future Work

In our previous experiments, 30% PTFE has been chosen as a carrier liquid. Teflon[®] solution has caused an increase in the conductivity of the PTFE dilution as it has been mixed with DI water. This results in a highly lossy surface. Finding a less lossy surfactant by diluting PTFE with another kind of liquid material instead of using water dispersed PTFE solutions will give us better inductance values.

The PDMS effect on PCB design will be investigated in a detailed way. In our previous test, we have observed the capacitive effect of PDMS block to the system. This capacitive effect should be minimized implementing better channel designs, since E field distribution on the microstrip transmission line is mainly between the copper lines and at the edges of the transmission line. Thus, rather than applying a microfluidic channel on the whole device, designing a fluidic channel on the transmission line will contribute to improvement of the inductance. To sum up, the effect of PDMS to the system should be analyzed carefully, and then the capacitive effect of the PDMS should be minimized decreasing the volume of PDMS block and planning different designs.

Although we have achieved a good and nonstop actuation of liquid metal in the closed loop channels, there still are some issues need to be improved such as

repeatability, accuracy and efficiency of actuation of liquid metal. A deeper investigation with various aspects of liquid metals and the environment of actuation is supposed to lead further insight to overcome all the problems and utilize liquid metals perfectly in modern devices.

REFERENCES

- [1] Q. Xu, N. Oudalov, Q. Guo, H. M. Jaeger, and E. Brown, "Effect of oxidation on the mechanical properties of liquid gallium and eutectic gallium-indium," *Physics of Fluids*, vol. 24, p. 063101, 2012.
- [2] K. Ma and J. Liu, "Liquid metal cooling in thermal management of computer chips," *Frontiers of Energy and Power Engineering in China*, vol. 1, pp. 384-402, 2007.
- [3] J. Kim, W. Shen, L. Latorre, and C.-J. Kim, "A micromechanical switch with electrostatically driven liquid-metal droplet," *Sensors and Actuators A: Physical*, vol. 97-98, pp. 672-679, 2002.
- [4] L. Tingyi, P. Sen, and K. Chang-Jin, "Characterization of nontoxic liquid-metal alloy galinstan for applications in microdevices," *Journal of Microelectromechanical Systems*, vol. 21, pp. 443-450, 2012.
- [5] M. Hodes, Z. Rui, R. Wilcoxon, and N. Lower, "Cooling potential of galinstan-based minichannel heat sinks," in *2012 13th IEEE Intersociety Conference on Thermal and Thermomechanical Phenomena in Electronic Systems (ITherm)*, pp. 297-302, 2012.
- [6] C. Chung-Hao, J. Whalen, and D. Peroulis, "Non-toxic liquid-metal 2-100 GHz MEMS switch," in *2007 IEEE/MTT-S International Microwave Symposium*, pp. 363-366, 2007.
- [7] S. Jalali Mazlouman, J. Xing Jie, A. Mahanfar, C. Menon, and R. G. Vaughan, "A reconfigurable patch antenna using liquid metal embedded in a silicone substrate," *IEEE Transactions on Antennas and Propagation*, vol. 59, pp. 4406-4412, 2011.
- [8] G. J. Hayes, S. Ju-Hee, A. Qusba, M. D. Dickey, and G. Lazzi, "Flexible liquid metal alloy (EGaIn) microstrip patch antenna," *IEEE Transactions on Antennas and Propagation*, vol. 60, pp. 2151-2156, 2012.
- [9] P. Yong-Lae, C. Bor-Rong, and R. J. Wood, "Design and fabrication of soft artificial skin using embedded microchannels and liquid conductors," *IEEE Sensors Journal*, vol. 12, pp. 2711-2718, 2012.
- [10] M. D. Dickey, R. C. Chiechi, R. J. Larsen, E. A. Weiss, D. A. Weitz, and G. M. Whitesides, "Eutectic gallium-indium (EGaIn): A liquid metal alloy for the

- formation of stable structures in microchannels at room temperature," *Advanced Functional Materials*, vol. 18, pp. 1097-1104, 2008.
- [11] M. R. Khan, G. J. Hayes, S. Zhang, M. D. Dickey, and G. Lazzi, "A pressure responsive fluidic microstrip open stub resonator using a liquid metal alloy," *IEEE Microwave and Wireless Components Letters*, vol. 22, pp. 577-579, 2012.
- [12] A. Qusba, A. K. RamRakhyani, S. Ju-Hee, G. J. Hayes, M. D. Dickey, and G. Lazzi, "On the design of microfluidic implant coil for flexible telemetry system," *IEEE Sensors Journal*, vol. 14, pp. 1074-1080, 2014.
- [13] D. M. Vogt, P. Yong-Lae, and R. J. Wood, "Design and characterization of a soft multi-axis force sensor using embedded microfluidic channels," *IEEE Sensors Journal*, vol. 13, pp. 4056-4064, 2013.
- [14] R. C. Chiechi, E. A. Weiss, M. D. Dickey, and G. M. Whitesides, "Eutectic gallium–indium (EGaIn): A moldable liquid metal for electrical characterization of self-assembled monolayers," *Angewandte Chemie International Edition*, vol. 47, pp. 142-144, 2008.
- [15] Q. Xu, N. Oudalov, Q. Guo, H. M. Jaeger, and E. Brown, "Effect of oxidation on the mechanical properties of liquid gallium and eutectic gallium-indium," *Physics of Fluids (1994-present)*, vol. 24, p. 063101, 2012.
- [16] J. Wang, S. Liu, S. Guruswamy, and A. Nahata, "Reconfigurable liquid metal based terahertz metamaterials via selective erasure and refilling to the unit cell level," *Applied Physics Letters*, vol. 103, p. 221116, 2013.
- [17] D. Kim, P. Thissen, G. Viner, D.-W. Lee, W. Choi, Y. J. Chabal, *et al.*, "Recovery of nonwetting characteristics by surface modification of gallium-based liquid metal droplets using hydrochloric acid vapor," *ACS Applied Materials & Interfaces*, vol. 5, pp. 179-185, 2012.
- [18] K. Daeyoung, L. Dong-weon, C. Wonjae, and L. Jeong-Bong, "A super-lyophobic 3-D PDMS channel as a novel microfluidic platform to manipulate oxidized galinstan," *Journal of Microelectromechanical Systems*, vol. 22, pp. 1267-1275, 2013.
- [19] Y. Kondoh, T. Takenaka, T. Hidaka, G. Tejima, Y. Kaneko, and M. Saitoh, "High-reliability, high-performance RF micromachined switch using liquid metal," *Journal of Microelectromechanical Systems*, vol. 14, pp. 214-220, 2005.

- [20] B. L. Cumby, G. J. Hayes, M. D. Dickey, R. S. Justice, C. E. Tabor, and J. C. Heikenfeld, "Reconfigurable liquid metal circuits by laplace pressure shaping," *Applied Physics Letters*, vol. 101, p. 174102, 2012.
- [21] G. Mumcu, A. Dey, and T. Palomo, "Frequency-agile bandpass filters using liquid metal tunable broadside coupled split ring resonators," *IEEE Microwave and Wireless Components Letters*, vol. 23, pp. 187-189, 2013.
- [22] L. Meng and N. Behdad, "Fluidically tunable frequency selective/phase shifting surfaces for high-power microwave applications," *IEEE Transactions on Antennas and Propagation*, vol. 60, pp. 2748-2759, 2012.
- [23] R. Kageyama, S. Kagami, M. Inaba, and H. Inoue, "Development of soft and distributed tactile sensors and the application to a humanoid robot," in *1999 IEEE SMC '99 Conference Proceedings*, vol. 2, pp. 981-986, 1999.
- [24] I. Zine-El-Abidine, M. Okoniewski, and J. G. McRory, "A tunable RF MEMS inductor," in *2004 International Conference on MEMS, NANO and Smart Systems*, pp. 636-638, 2004.
- [25] S. Chang and S. Sivoththaman, "A tunable RF MEMS inductor on silicon incorporating an amorphous silicon bimorph in a low-temperature process," *IEEE Electron Device Letters*, vol. 27, pp. 905-907, 2006.
- [26] I. El Gmati, P. Calmon, R. Fulcrand, P. Pons, A. Boukabache, H. Boussetta, "Variable RF MEMS fluidic inductor incorporating lamination process," *IET Micro & Nano Letters*, vol. 5, pp. 370-373, 2010.
- [27] A. Fassler and C. Majidi, "Soft-matter capacitors and inductors for hyperelastic strain sensing and stretchable electronics," *Smart Materials and Structures*, vol. 22, p. 055023, 2013.
- [28] S. Cheng and Z. Wu, "A microfluidic, reversibly stretchable, large-area wireless strain sensor," *Advanced Functional Materials*, vol. 21, pp. 2282-2290, 2011.
- [29] R. K. Kramer, C. Majidi, and R. J. Wood, "Masked deposition of gallium-indium alloys for liquid-embedded elastomer conductors," *Advanced Functional Materials*, vol. 23, pp. 5292-5296, 2013.
- [30] A. M. Okamura and M. R. Cutkosky, "Feature detection for haptic exploration with robotic fingers," *The International Journal of Robotics Research*, vol. 20, pp. 925-938, 2001.

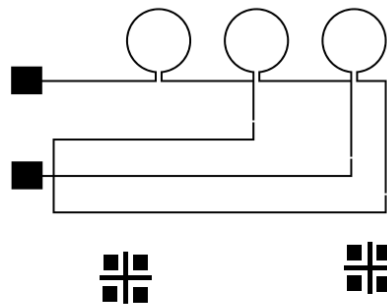
- [31] B. J. Lei, H. Wenqi, A. T. Ohta, and W. A. Shiroma, "A liquid-metal reconfigurable double-stub tuner," in *2012 IEEE MTT-S International Microwave Symposium Digest (MTT)*, pp. 1-3, 2012.
- [32] Y. Ito, Y. Yoshihara, H. Sugawara, K. Okada, and K. Masu, "A 1.3-2.8 GHz wide range CMOS LC-VCO using variable inductor," in *2005 Asian Solid-State Circuits Conference*, pp. 265-268, 2005.
- [33] I. El Gmati, R. Fulcrand, P. Calmon, A. Boukabache, P. Pons, H. Boussetta, "RF MEMS fluidic variable inductor," in *2010 5th International Conference on Design and Technology of Integrated Systems in Nanoscale Era (DTIS)*, pp. 1-3, 2010.
- [34] K. Ohashi, Y. Ito, Y. Yoshihara, K. Okada, and K. Masu, "A wideband CMOS LC-VCO using variable inductor," in *2007 ASP-DAC Asia and South Pacific Design Automation Conference*, pp. 98-99, 2007.
- [35] G. Li, M. Parmar, D. Kim, J.-B. Lee, and D.-W. Lee, "PDMS based coplanar microfluidic channels for the surface reduction of oxidized galinstan," *Lab on a Chip*, vol. 14, pp. 200-209, 2014.
- [36] S. Cheng and Z. Wu, "Microfluidic electronics," *Lab on a Chip*, vol. 12, pp. 2782-2791, 2012.
- [37] 3M. "3M™ Novec™ 2702 electronic grade coating." Internet: <http://www.multimedia.3m.com>, Oct., 2013 [May 01, 2014].
- [38] Z. Wu and K. Hjort, "Surface modification of PDMS by gradient-induced migration of embedded pluronic," *Lab on a Chip*, vol. 9, pp. 1500-1503, 2009.
- [39] J. Zhou, D. A. Khodakov, A. V. Ellis, and N. H. Voelcker, "Surface modification for PDMS-based microfluidic devices," *Electrophoresis*, vol. 33, pp. 89-104, 2012.
- [40] D. K. Cheng. *Field and Wave Electromagnetics*, 2nd ed. Reading, MA: Addison-Wesley, 1989, pp. 320-322.
- [41] 3M. "3M™ Novec™ 4300 electronic surfactant." Internet: <http://www.multimedia.3m.com>, Sept., 2013 [May 01, 2014].

APPENDIX A

Mask and 3D Master Mold Designs

A.1.Mask Designs

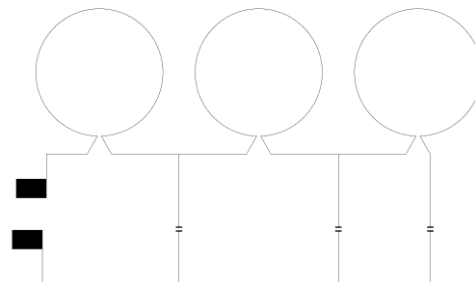
2013-12-07 Inductor conductive layer Yusuf Dogan



Texas A&M Univ. NanoBio Systems Lab.

Figure A.1.1: Type 1 Loop Inductor

2014-02-04 planar loop inductor Yusuf Dogan



Texas A&M Univ. NanoBio Systems Lab.

Figure A.1.2: Type 2 Loop Inductor

A.2. 3D Master Mold Designs

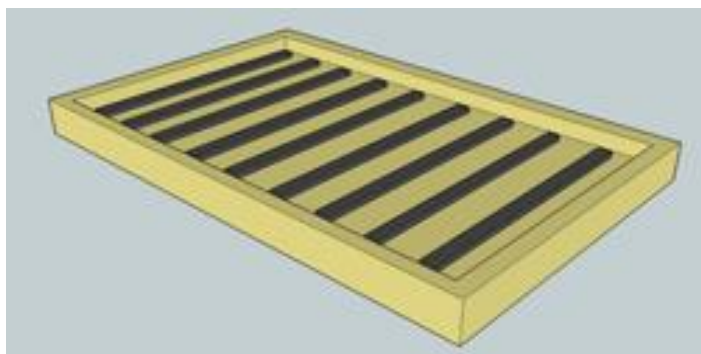


Figure A.2.1: 2mm Width 1mm Height Straight Channel Mold for Coating and Surfactant Tests

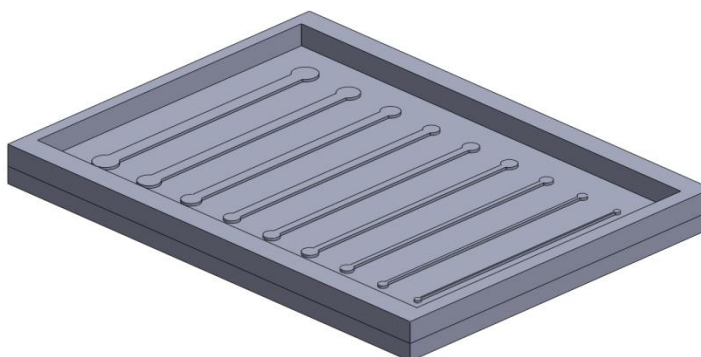


Figure A.2.2: Different Dimension Straight Channel Master Mold Design

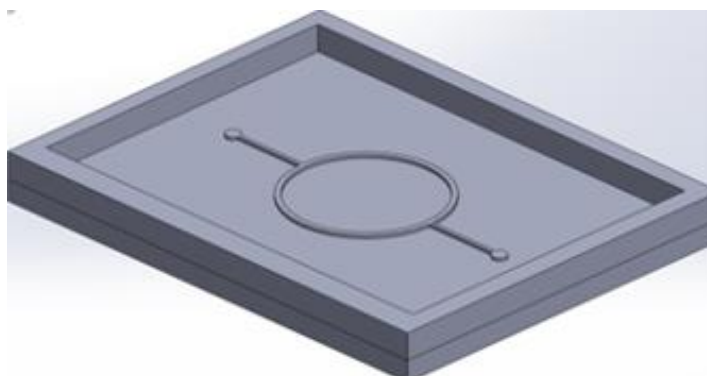


Figure A.2.3: Closed Loop Channel Master Mold Design

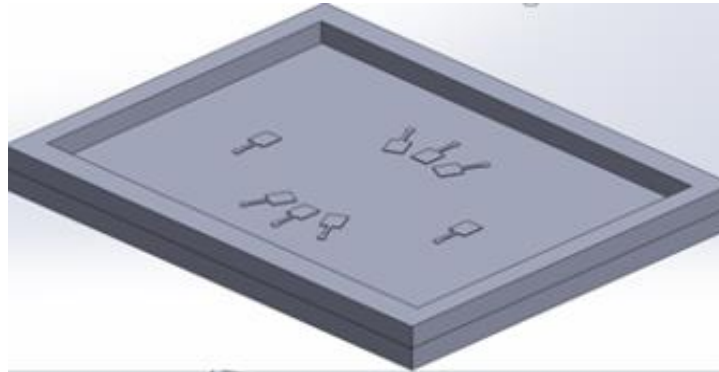


Figure A.2.4: Closed Loop Valve Layer Master Mold Design

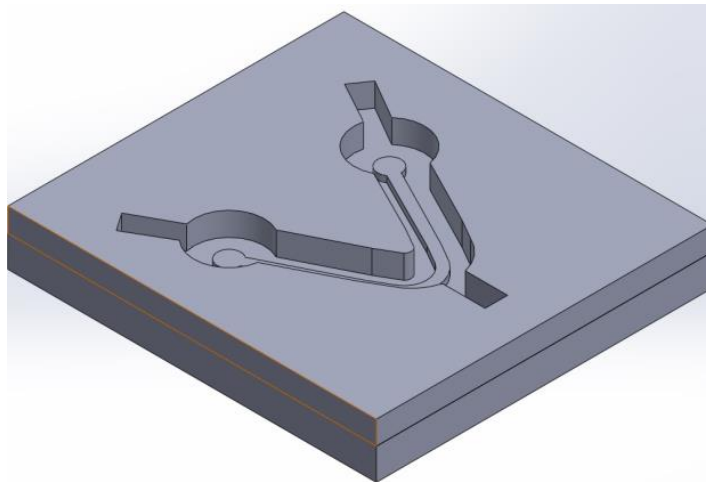


Figure A.2.5: Straight Channel Master Mold Design for PCB Inductor

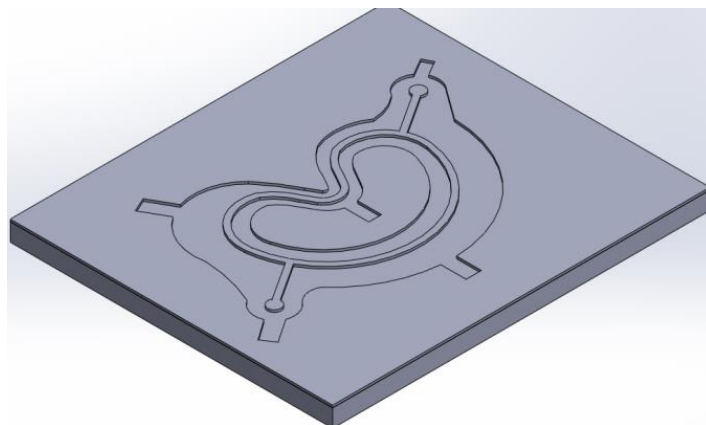


Figure A.2.6: Closed Loop Channel Master Mold Design for PCB

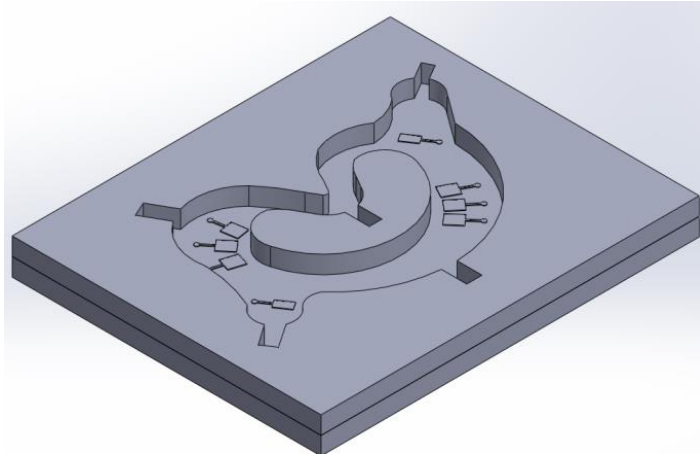


Figure A.2.7: Closed Loop Valve Layer Master Mold Design for PCB

APPENDIX B

Loop Inductor Fabrication Procedure

B.1. Loop Inductor Patterning Procedure

1. Clean the 2x3 inch glass slide with acetone, IPA, and DI water in sequence and dry with N₂ gas
2. Dehydrate baking at 200°C for 10 minutes
3. Deposit Cr/Cu layer using an E-beam evaporator to a thickness of 2000 Å
4. Repeat steps 1 and 2
5. Spin coat Futurex[®] NR21-20000P negative photoresist (Futurex[®] Inc. Franklin, NJ.) on the glass slide at 2000 rpm for 40 seconds with an acceleration time of 5 seconds
6. Soft baking at 140°C for 7 minutes, cool down
7. Expose UV using a mask electrode design (MJB3, SUSS MicroTec Inc., Waterbury
8. Center, VT) at 17 mW/cm² (wavelength: 320 nm) for 117 second
9. Post exposure baking at 85°C for 6 minutes, cool down
10. Develop the pattern using RD-6 developer (Futurex[®] Inc. Franklin, NJ) for 90-120 seconds
11. Rinse in DI water and dry with N₂ gas. Only the copper inductor and transmission line will be opened
12. Electroplate copper on the patterned region (B.2 will lead you)
13. Take out the negative resist using acetone or RR4 resist remover (Futurex[®] Inc. Franklin, NJ) till all the negative resist is gone
14. Rinse with DI water and dry with N₂ gas
15. Etch with copper etchant for about 2-3 seconds

16. Rinse with DI water
17. Etch with chromium etchant for about 20-30 seconds or use diluted HCl and some aluminum foil for about 5-10 seconds
18. Rinse the glass slide with DI water, acetone, IPA, and DI water in sequence, and dry with N₂ gas

B.2. Copper Electroplating on Patterned Loop Design

1. Place a metal plate and your sample at the stand (Do not change the fixed distance between the plate and sample)
2. Connect '+' wire (red color) of the power supply to the metal plate and '-' wire (green color) of the power supply to your sample
3. Place a beaker on the hotplate and pour electroplating solution and put a magnetic bar to stir the solution (Set the stirrer speed at 90 RPM)
4. Turn on the power supply
5. Set the total run time
6. Set the current (using the density of 10 mA/cm²)
7. To run the electroplating, press OPR button
8. If the displayed voltage is high and the displayed current is 0.001, it means there is no current flow. Check the electric wire connection and your sample
9. If you want to pause or stop the electroplating, press STBY button
10. Once the run is over, press STBY button and turn off the power supply
11. Take out the metal plate and your sample. Wash them with DI water and dry them with N₂ gas
12. Pour the electroplating solution into the container and rinse the beaker with DI water
13. Clean out the area you used

APPENDIX C

PDMS Device Fabrication Procedure

C.1. Glass and PCB Inductor Devices with Straight Microfluidic Channel

C.1.1. 60 μ m PDMS Layer on PMMA

1. Mix PDMS (Sylgard® 184, Dow Corning, Inc., Midland, MI) prepolymer with curing agent at 10:1 ratio, and degas in a desiccator for 10 minutes
2. Pour 3g degassed PDMS prepolymer mixture onto the cleaned PMMA, and degas again in the desiccator for 10 minutes
3. Spin coat at 2000 rpm for 40 seconds
4. Cure in an 65°C oven for 8 hours

C.1.2. Microchannel PDMS Block Layer Fabrication

1. Place the fabricated 3D master molds inside the desiccator together with a weight boat containing 6~7 drops of tridecafluoro-1,1,2,2-tetrahydrooctyl (trichlorosilane, United Chemical Technologies, Inc., Bristol, PA)
2. Vacuum the desiccator for 10 min to allow trichlorosilane vaporize and be evenly sprayed over the molds
3. Mix PDMS (Sylgard® 184, Dow Corning, Inc., Midland, MI) prepolymer with curing agent at 10:1 ratio, and degas in a desiccator for 10 minutes
4. Pour the degassed PDMS prepolymer mixture onto trichlorosilane coated master molds for 10-20g per each mold, and degas again in the desiccator for 30 minutes
5. Cure in a 65°C oven for 8 hours

C.1.3. PDMS device bonding

1. Peel off the cured PDMS block layer
2. Punch holes in the valve layer block with 1.5 mm biopsy punch (Acuderm Inc., Ft. Lauderdale, FL)

3. Apply oxygen plasma treatment (100 mTorr, 100W, 90 sec) for both PDMS spin coated PMMA and channel layer block
4. Bond those under a stereo microscope

C.2. Closed Loop Channel Device Fabrication

C.2.1. PDMS Block Fabrication for Liquid and Valve Layer

(Apply the steps of C.1.2)

C.2.2. 25 μ m PDMS Membrane Fabrication Procedure

1. Place bare Si wafer inside the desiccator with a weight boat containing 6~7 drops of tridecafluoro-1,1,2,2-tetrahydrooctyl (trichlorosilane, United Chemical Technologies, Inc., Bristol, PA)
2. Vacuum the desiccator for 10 min to allow trichlorosilane vaporize and be evenly sprayed over the wafer
3. Mix PDMS (Sylgard® 184, Dow Corning, Inc., Midland, MI) prepolymer with curing agent at 10:1 ratio, and degas in a desiccator for 10 minutes
4. Pour 3g degassed PDMS prepolymer mixture onto trichlorosilane coated wafer, and degas again in the desiccator for 10 minutes
5. Spin coat at 3000 rpm for 40 seconds
6. Cure in an 85°C oven for 2 hours

C.2.3. PDMS device bonding

1. PDMS valve layer and membrane bonding (Apply the steps of C.1.3)
2. Peel off the bonded device from Si wafer
3. Punch inlet and outlet holes in the valve layer block with 1.5 mm biopsy punch (Acuderm Inc., Ft. Lauderdale, FL)
4. PDMS liquid channel layer and membrane bonding (Apply the steps of C.1.3)

C.3. PCB Inductor Device with Closed Loop Channel

C.3.1. 60 μ m PDMS Layer on PCB Inductor

(Apply the steps of C.1.1)

C.3.2. 25 μ m PDMS Membrane Fabrication Procedure

(Apply the steps of C.2.2)

C.3.3. PDMS Block Fabrication for Valve Layer

(Apply the steps of C.1.2)

C.3.4. PDMS Device Bonding

1. Mix PDMS (Sylgard® 184, Dow Corning, Inc., Midland, MI) prepolymer with curing agent at 10:1 ratio, and degas in a desiccator for 10 minutes
2. Pour 10g degassed PDMS prepolymer mixture onto liquid channel master mold, and degas again in the desiccator for 10 minutes
3. Put the PDMS valve layer block which is already bonded with 25 μ m PDMS membrane on the liquid channel master mold that has uncured PDMS on it
4. Align and press down with weight blocks by means of parafilm between the weight and PDMS block
5. Cure in an 65°C oven for 8 hours
6. Peel off the all bonded PDMS device from liquid channel master mold
7. Bond with already 60 μ m PDMS coated PCB inductor by using oxygen plasma treatment (100 mTorr, 100W, 90 sec)

APPENDIX D

Operation Control

D.1. Peristaltic Pump Controlling Platform

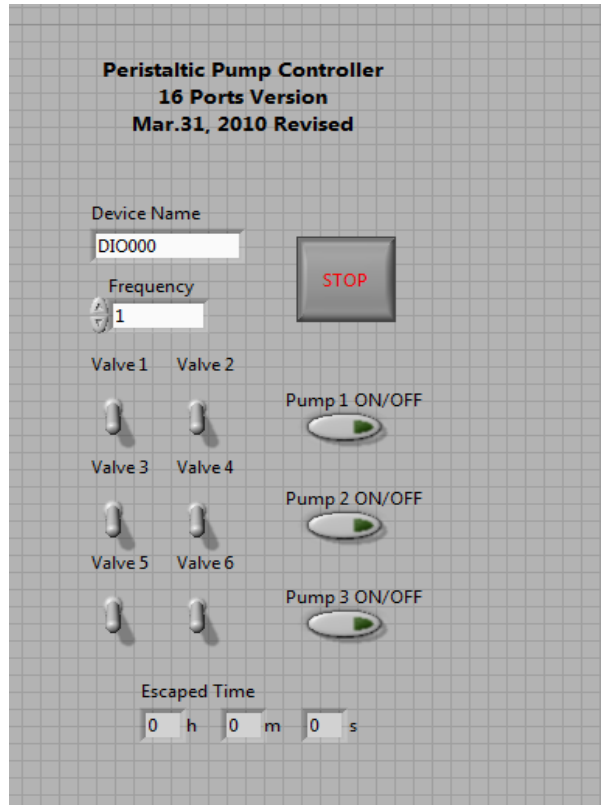


Figure D.1: Front Panel of the LabVIEW™ Program for Peristaltic Pump Controlling.

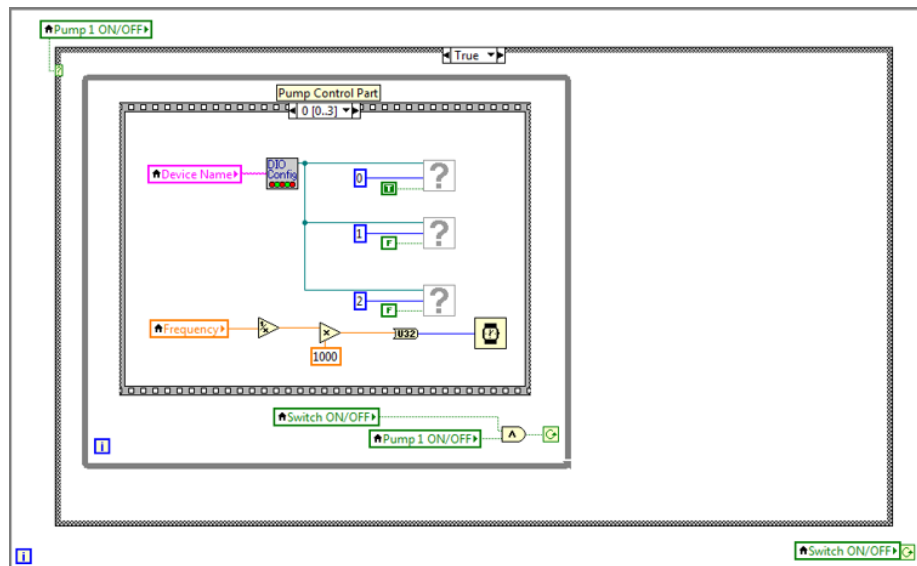
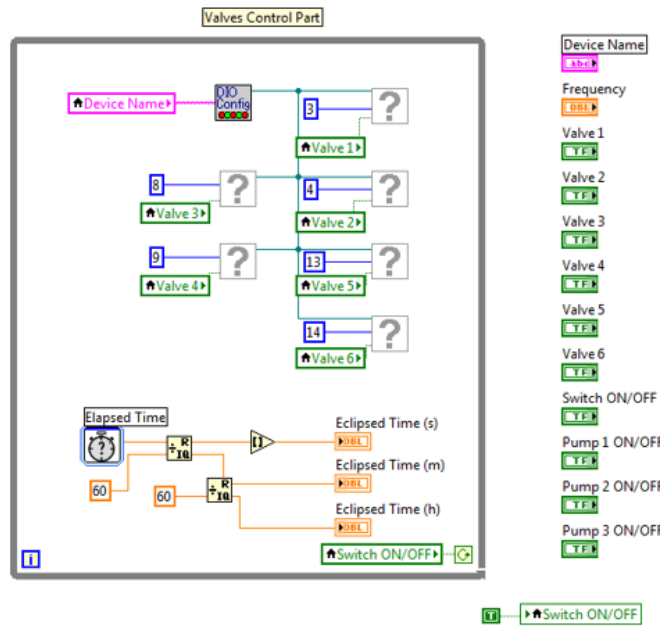


Figure D.2: Block Diagram of the LabVIEW™ Program for Peristaltic Pump Controlling.